
000 FROM RISK TO UNCERTAINTY:
001 GENERATING PREDICTIVE UNCERTAINTY MEASURES
002 VIA BAYESIAN ESTIMATION
003
004
005

006 **Anonymous authors**

007 Paper under double-blind review
008
009

010
011 ABSTRACT
012

013 There are various measures of predictive uncertainty in the literature, but their
014 relationships to each other remain unclear. This paper uses a decomposition
015 of statistical pointwise risk into components, associated with different sources
016 of predictive uncertainty, namely aleatoric uncertainty (inherent data variability)
017 and epistemic uncertainty (model-related uncertainty). Together with Bayesian
018 methods, applied as an approximation, we build a framework that allows one
019 to generate different predictive uncertainty measures. We validate our method
020 on image datasets by evaluating its performance in detecting out-of-distribution
021 and misclassified instances using the AUROC metric. The experimental results
022 confirm that the measures derived from our framework are useful for the considered
023 downstream tasks.

024
025 1 INTRODUCTION
026

027 Nowadays, predictive models are applied in a variety of fields requiring high-risk decisions such as
028 medical diagnosis (Shen et al., 2017; Litjens et al., 2017), finance (Ozbayoglu et al., 2020; Heaton
029 et al., 2017), autonomous driving (Grigorescu et al., 2020; Mozaffari et al., 2020) and others. A
030 careful analysis of model predictions is required to mitigate the risks. Hence, it is of high importance
031 to evaluate the predictive uncertainty of the models. In recent years, a variety of approaches to
032 quantify predictive uncertainty have been proposed (Kotelevskii et al., 2022; Lahlou et al., 2023;
033 Kendall & Gal, 2017; Van Amersfoort et al., 2020; Liu et al., 2020a; Lakshminarayanan et al., 2017;
034 Malinin & Gales, 2021; Schweighofer et al., 2023a;b) and others. Specific attention has been paid
035 to the distinction between different sources of uncertainty. It is commonly agreed to consider two
036 sources of uncertainty (Hüllermeier & Waegeman, 2021): **aleatoric** uncertainty, that effectively
037 reduces to the inherent [stochastic relationship between the inputs \(objects\) and the outputs \(labels\)](#),
038 and **epistemic** uncertainty, which is referred to as the uncertainty due to the “lack of knowledge”
039 about the true data distribution. Distinguishing between aleatoric and epistemic uncertainties is
040 crucial in practice because it helps identifying whether uncertainty can be reduced by gathering more
041 data (epistemic) or if it is inherent to the problem (aleatoric), thus guiding better decision-making
042 and model improvement.

043 Despite the practical importance and widespread usage of uncertainty quantification, *there is still*
044 *no common strict formal definition of both types of uncertainty*. This leads to a number of different
045 measures to quantify either type of uncertainty (see for example (Lakshminarayanan et al., 2017;
046 Gal et al., 2017; Malinin & Gales, 2021; Hüllermeier & Waegeman, 2021; Kotelevskii et al., 2022;
047 Schweighofer et al., 2023a)). [Recently, for information-theoretical measures, the step towards unified](#)
048 [definition was made in \(Schweighofer et al., 2023a\)](#). However, it is not clear how all these measures
049 of uncertainty are related to each other [in general](#). Do they complement or contradict each other?
050 Are they special cases of some general class of measures? In this paper, we introduce a statistical
051 approach for predictive uncertainty quantification, reasoning in terms of pointwise risk estimation.
052 This allows us to reconstruct a lot of known and popular measures of predictive uncertainty, as well
053 as show how to build new ones. Our contributions are as follows:

1. [Following \(Kotelevskii et al., 2022; Lahlou et al., 2023; Liu et al., 2019\)](#), we consider pointwise risk decomposition into distinct parts, that are responsible for capturing different

sources of uncertainty. We show, that this decomposition, applied specifically to strictly proper scoring rules (Gneiting & Raftery, 2007; Gruber & Buettner, 2023) leads to a general framework, that is amenable for generation of uncertainty measures.

2. We show how one can make this framework practical with the help of Bayesian estimation (see Section 4). We show that commonly used measures of epistemic uncertainty, such as Mutual Information (Houlsby et al., 2011; Gal et al., 2017), Expected Pairwise Kullback-Leibler divergence (EPKL) (Schweighofer et al., 2023a; Malinin & Gales, 2018), predictive variance and maximum probability score are special cases within our general approach. We also highlight the limitations of our framework, elaborating on discussions from (Schweighofer et al., 2023a; Wimmer et al., 2023).
3. We experimentally evaluate different predictive uncertainty quantification measures from the proposed framework in various tasks. Specifically, we consider out-of-distribution detection and misclassification detection; see Section 6. Our results highlight the conditions under which each measure is most effective, providing practical insights for selecting appropriate uncertainty measures.

2 PREDICTIVE UNCERTAINTY QUANTIFICATION VIA RISKS

Assume we have a dataset $D_{tr} = \{(X_i, Y_i)\}_{i=1}^N$, where pairs $X_i \in \mathbb{R}^d, Y_i \in \mathcal{Y}$ are i.i.d. random variables sampled from a joint training distribution $P_{tr}(X, Y)$. We consider a classification task over K classes, i.e. $\mathcal{Y} = \{1, \dots, K\}$. We can express this joint distribution as a product: $P_{tr}(X, Y) = P_{tr}(Y | X)P_{tr}(X)$.

In practice, we typically consider a parametric model $P(Y | X, \theta)$ with parameters θ to approximate $P_{tr}(Y | X)$. We denote the true class probabilities for an input x as $\eta(x) = P_{tr}(Y | X = x)$, and the predicted probabilities as $\eta_\theta(x) = P(Y | X = x, \theta)$. We will often omit the index θ and denote the predicted probability vector by $\hat{\eta}$.

2.1 POINTWISE RISK AS A MEASURE OF UNCERTAINTY

The goal of uncertainty quantification is to measure the degree of confidence of predictive models, distinguishing between aleatoric and epistemic sources of uncertainty. In the paper, following (Kotelevskii et al., 2022; Lahlou et al., 2023), we introduce uncertainty via the statistical concept of risk.

In machine learning, the main concern is the model’s “error” at a particular input point x . One way to express this error is through the expected risk. Let $\ell: \mathbb{R}^K \times \mathcal{Y} \rightarrow \mathbb{R}$ be a loss function that measures how well $\hat{\eta}(x)$ matches the true label y . The pointwise risk $R(\eta, \hat{\eta} | x)$ for a model $\hat{\eta}$ is defined as:

$$R(\eta, \hat{\eta} | x) = \int \ell(\hat{\eta}(x), y) dP(y | X = x). \quad (1)$$

Thus, pointwise risk is an expected loss received by a specific predictor $\hat{\eta}$ at a particular input point x . Importantly, pointwise risk, while being a natural measure of expected model error, can not be used directly as a measure of uncertainty as it is not possible to compute it due to unknown true data distribution. We will discuss possible ways to transform pointwise risk into the practical uncertainty measure in Section 4.

Note, that we use distribution P , which might differ from P_{tr} . If $P(X) \neq P_{tr}(X)$ but $P(Y | X = x) = P_{tr}(Y | X = x)$ for any x , this situation is called “covariate shift”. We consider this setup and assume $\eta(x) = P(Y | X = x)$ is *valid* for any x , meaning it is a vector of length K regardless of the input. Limitations of this assumption are discussed in Appendix B.

2.2 ALEATORIC AND EPISTEMIC UNCERTAINTIES VIA RISKS

Predictive uncertainty can be divided into two parts. **Aleatoric** uncertainty expresses the degree of ambiguity in data and does not depend on the model, being an inherent property of the data given a particular choice of feature representation. **Epistemic** uncertainty is vaguely defined but typically is associated with the “lack of knowledge” of choosing the right model parameters θ and

108 **model misspecification**. When the source of uncertainty is not important, practitioners consider **total**
 109 uncertainty that aggregates all the sources.

110 Pointwise risk allows for the following decomposition:

$$111 \underbrace{\mathbf{R}(\eta, \hat{\eta} | x)}_{\text{Total risk}} = \underbrace{\mathbf{R}_{\text{Bayes}}(\eta | x)}_{\text{Bayes risk}} + \underbrace{\mathbf{R}(\eta, \hat{\eta} | x) - \mathbf{R}_{\text{Bayes}}(\eta | x)}_{\text{Excess risk}}, \quad (2)$$

112 where $\mathbf{R}_{\text{Bayes}}$ is the pointwise Bayes risk, defined as:

$$113 \mathbf{R}_{\text{Bayes}}(\eta | x) = \int \ell(\eta(x), y) dP(y | X = x).$$

114 The Bayes risk represents the expected error from the true data-generative process $\eta(x)$. It does
 115 not depend on the parameters of the model nor the choice of model architecture, and hence can
 116 be seen as a measure of *aleatoric* uncertainty. **Note that in our analysis, we treat x as a noiseless**
 117 **observed variable. Alternatively, one could assume that only noisy observations \tilde{x} are available and**
 118 **include the uncertainty in observations into the definition of aleatoric uncertainty. However, we do**
 119 **not explore this scenario in this work.** The second term in equation (2) is ‘‘Excess risk’’ and represents
 120 the difference between the risks computed for the approximation and for the true model at a given
 121 input point x . Thus, it naturally represents a lack of knowledge about the true data distribution, i.e.
 122 *epistemic* uncertainty. We note that decomposition (2) was previously considered in the context of
 123 uncertainty quantification in (Kotelevskii et al., 2022; Lahlou et al., 2023).

124 Although the decomposition (2) is useful, it doesn’t provide much information about the properties of
 125 these risk functions in general cases. Therefore, we consider a specific class of loss functions, strictly
 126 proper scoring rules, which allows us to do a theoretical analysis.

132 3 RISKS FOR STRICTLY PROPER SCORING RULES

133 **Strictly proper scoring rules** (Gneiting & Raftery, 2007) represent a class of loss functions that
 134 ensure that the minimizing predictive distributions coincide with the data-generating distribution
 135 $P(Y | X)$. Let’s say a forecaster can produce a vector of predicted probabilities $P \in \mathcal{P}_K$, where \mathcal{P}_K
 136 is a space of discrete probability distributions over K classes. Then, $\ell(P, y) : \mathcal{P}_K \times \mathcal{Y} \rightarrow \mathbb{R}$ is the
 137 penalty the forecaster would have, given that event y is materialized. Its expected value with respect
 138 to some distribution Q we will denote as $\ell(P, Q) = \int \ell(P, y) dQ(y)$.

139 A scoring rule is called *strictly proper* if, for any $P, Q \in \mathcal{P}_K$, it satisfies the condition $\ell(P, Q) \geq$
 140 $\ell(Q, Q)$, with equality holding only when $P = Q$. Under mild assumptions (see Theorem 3.2
 141 in (Gneiting & Raftery, 2007)), any strictly proper scoring rule can be represented as:

$$142 \ell(\eta, y) = \langle G'(\eta), \eta \rangle - G'_y(\eta) - G(\eta),$$

143 where $\langle \cdot, \cdot \rangle$ is a scalar product, $G : \mathcal{P}_K \rightarrow \mathbb{R}$ is a strictly convex function, and $G'(\eta) =$
 144 $\{G'_1(\eta), \dots, G'_K(\eta)\}$ is a vector of element-wise subgradients.

145 **Risk decompositions for strictly proper scoring rules.** Here we derive the explicit expressions for
 146 different types of risks for strictly proper scoring rules (detailed derivations are given in Appendix C).

- 147 • **Total Risk (Total Uncertainty):**

$$148 \mathbf{R}_{\text{Tot}}(\eta, \hat{\eta} | x) = \langle G'(\hat{\eta}), \hat{\eta} \rangle - G(\hat{\eta}) - \langle G'(\hat{\eta}), \eta \rangle. \quad (3)$$

149 Note, that Total risk depends *linearly* on the true data generative distribution η .

- 150 • **Bayes Risk (Aleatoric Uncertainty):**

$$151 \mathbf{R}_{\text{Bayes}}(\eta | x) = -G(\eta). \quad (4)$$

152 Note, that Bayes risk is a concave function of η , since function G is convex.

- 153 • **Excess risk (Epistemic Uncertainty):**

$$154 \mathbf{R}_{\text{Exc}}(\eta, \hat{\eta} | x) = D_G(\eta \| \hat{\eta}), \quad (5)$$

155 where $D_G(\eta \| \hat{\eta}) = G(\eta) - G(\hat{\eta}) - \langle G'(\hat{\eta}), \eta - \hat{\eta} \rangle$ is Bregman divergence (Bregman,
 156 1967).

	Log score	Brier score	Zero-one score	Spherical score
$G(\eta)$	$\sum_{k=1}^K \eta_k \log \eta_k$	$-\sum_{k=1}^K \eta_k (1 - \eta_k)$	$\max_k \eta_k - 1$	$\ \eta\ _2 - 1$
$\bar{\eta}$	$\frac{\exp \mathbb{E} \log \eta}{\sum_{k'} (\exp \mathbb{E} \log \eta)_{k'}}$	$\mathbb{E} \eta$	Not defined	$\ x_0\ _2 \left[n + \frac{m}{\sqrt{1 - \ m\ _2^2}} \right]$
Aleatoric (Bayes risk)	$\mathbb{H} \eta$	$1 - \ \eta\ _2^2$	$1 - \max_k \eta_k$	$1 - \ \eta\ _2$
Epistemic (Excess risk)	$D_{\text{KL}}[\eta \ \hat{\eta}]$	$\ \eta - \hat{\eta}\ _2^2$	$\max_k \eta_k - \eta_{\arg \max_k \hat{\eta}_k}$	$\ \eta\ _2 (1 - \langle \frac{\hat{\eta}}{\ \hat{\eta}\ _2}, \frac{\eta}{\ \eta\ _2} \rangle)$
Total (Risk)	$\text{CE}[\eta \ \hat{\eta}]$	$\ \eta - \hat{\eta}\ _2^2 - \ \eta\ _2^2 + 1$	$1 - \eta_{\arg \max_k \hat{\eta}_k}$	$1 - \ \eta\ _2 \langle \frac{\hat{\eta}}{\ \hat{\eta}\ _2}, \frac{\eta}{\ \eta\ _2} \rangle$

Table 1: Expressions for risks and central predictions, computed for different strictly proper scoring rules. We omitted x for clarity. D_{KL} stands for Kullback-Leibler divergence and CE for Cross-Entropy. See Section D for full derivations of risk instantiations and Section L for central predictions.

In what follows, we will assume the dependency of risks on $\eta, \hat{\eta}$ and for clarity will omit it, writing it as a function of x instead.

Specific Instances of Proper Scoring Rules. Different choices of the convex function G lead to different proper scoring rules. Table 1 shows the results for some popular cases often used in machine learning algorithms (see detailed derivations in Appendix D).

From Table 1, we see, that some of the risks correspond to well-known aleatoric uncertainty measures. For example, the Bayes risk for the Log score is given by the entropy of the predictive distribution. For the Zero-one score, this component is given by the so-called MaxProb, also widely applied (Geifman & El-Yaniv, 2017; Kotelevskii et al., 2022; Lakshminarayanan et al., 2017). For the Excess risk, we obtain different examples of Bregman divergence which lead to some well-known uncertainty measures when coupled with the Bayesian approach to risk estimation (see Section 4).

Estimating risks. The derived equations are useful but require access to the true data-generative distribution η , which is typically unknown. One approach to deal with this problem was introduced in (Kotelevskii et al., 2022), where authors considered a specific model η_θ , namely Nadaraya-Watson kernel regression, as it has useful asymptotic properties to approximate Excess risk. Another approach, the DEUP (Lahlou et al., 2023) proposed a method for estimating Excess risk by directly training a model to predict errors. However, in general cases, it is hardly possible to derive these results. In this paper, we consider a Bayesian approach to approximate η that allows us to derive both well-known from the literature and new uncertainty measures based on one unified framework.

4 BAYESIAN RISK ESTIMATION

The derived equations for risks depend on the true data generative distribution η and on some approximation of it $\hat{\eta}$. In particular, η appears in all the risks and is unknown. One needs to deal with that to obtain a computable uncertainty measure. In the Bayesian paradigm, one considers a posterior distribution over model parameters $p(\theta \mid D_{tr})$ that immediately leads to a distribution over predictive distributions $\eta_\theta \mid D_{tr}$. The goal of this section is to give a complete recipe for risk estimation under the Bayesian approach.

One can think of the risks as functions of η and $\hat{\eta}$, namely $g(\eta, \hat{\eta})$, where g is a shortcut for any risk function (Bayes risk is a function of only one argument). We can approximate the risks with the help of posterior distribution using one of three ideas:

1. **Bayesian averaging of risk.** One can consider $\mathbb{E}_\theta g(\eta_\theta, \hat{\eta})$ to approximate an impact of the true model η . In a fully Bayesian paradigm, the same can be done with $\hat{\eta}$ leading to the fully Bayesian risk estimate $\mathbb{E}_\theta \mathbb{E}_{\hat{\eta}} g(\eta_{\hat{\eta}}, \eta_\theta)$.
2. **Central label** (Posterior predictive distribution). One may use posterior predictive distribution $\hat{\eta}_{D_{tr}} = \arg \min_z \mathbb{E}_\theta D_G(\eta_\theta \parallel z) = \mathbb{E}_\theta \eta_\theta$ and plug it in risk equations instead of η and/or $\hat{\eta}$. This estimate naturally appears in decompositions of Bregman divergences (Pfau, 2013; Adlam et al., 2022), and in this context it is called ‘‘central label’’.
3. **Central prediction.** Interestingly, there is another natural estimate, that appears in the literature on Bregman divergences (Pfau, 2013; Adlam et al., 2022; Gruber & Buettner, 2023) and is referred to as ‘‘central prediction’’. It is defined as $\bar{\eta} = \arg \min_z \mathbb{E}_\theta D_G(z \parallel \eta_\theta)$.

216 In general, one can consider nine approximations of Excess and Total risks (three approximation
 217 options for each of the two arguments) and three of Bayes risk. We denote the specific type of
 218 approximation listed above by positional indices 1, 2 and 3. For example, $\tilde{g}^{(1,1)} = \mathbb{E}_{\tilde{\theta}} \mathbb{E}_{\theta} g(\eta_{\tilde{\theta}}, \eta_{\theta})$,
 219 $\tilde{g}^{(3,1)} = \mathbb{E}_{\theta} g(\tilde{\eta}, \eta_{\theta})$, and so on.

221 In this section, we present some of the formulas for the resulting aleatoric, and epistemic uncer-
 222 tainty measures with brief remarks on different approximations. For detailed derivations, other
 223 approximation options (not listed in the main part) and discussions, refer to Appendix E.

224 For **Bayes risk** we obtain three cases as it doesn't depend on $\hat{\eta}$:

225
 226
$$\tilde{\mathbf{R}}_{\text{Bayes}}^{(1)}(x) = -\mathbb{E}_{\theta} G(\eta_{\theta}), \quad \tilde{\mathbf{R}}_{\text{Bayes}}^{(2)}(x) = -G(\hat{\eta}_{D_{tr}}) \quad \text{and} \quad \tilde{\mathbf{R}}_{\text{Bayes}}^{(3)}(x) = -G(\tilde{\eta}).$$

227
 228 For **Excess risk** we obtain the whole family of approximations. We list some of them here (see others
 229 in Appendix E):

230
 231 • **Expected Pairwise Bregman Divergence (EPBD):**

232
 233
$$\tilde{\mathbf{R}}_{\text{Exc}}^{(1,1)}(x) = \mathbb{E}_{\tilde{\theta}} \mathbb{E}_{\theta} D_G(\eta_{\tilde{\theta}} \parallel \eta_{\theta}).$$

234 In a special case of Log score, it is an Expected Pairwise KL (EPKL; Malinin & Gales
 235 (2021); Schweighofer et al. (2023a)).

236
 237 • **Bregman Information (BI):**

238
 239
$$\tilde{\mathbf{R}}_{\text{Exc}}^{(1,2)}(x) = \mathbb{E}_{\theta} D_G(\eta_{\theta} \parallel \hat{\eta}_{D_{tr}}).$$

240 In a special case of Log score, it is Mutual Information (Gal et al., 2017; Houlby et al.,
 241 2011; Malinin & Gales, 2018). In case of Brier score, it is sum of predictive variances
 242 (class-wise).

243
 244 • **Reverse Bregman Information (RBI):**

245
 246
$$\tilde{\mathbf{R}}_{\text{Exc}}^{(2,1)}(x) = \mathbb{E}_{\theta} D_G(\hat{\eta}_{D_{tr}} \parallel \eta_{\theta}).$$

247 Its special case for Log score is known as Reverse Mutual Information (RMI; Malinin &
 248 Gales (2021)).

249
 250 • **Modified Bregman Information (MBI):**

251
 252
$$\tilde{\mathbf{R}}_{\text{Exc}}^{(1,3)}(x) = \mathbb{E}_{\theta} D_G(\eta_{\theta} \parallel \tilde{\eta}).$$

253 It is similar to Bregman Information, but the deviation is computed from the ‘‘central
 254 prediction’’, not the central label (BMA).

255
 256 • **Modified Reverse Bregman Information (MRBI):**

257
 258
$$\tilde{\mathbf{R}}_{\text{Exc}}^{(3,1)}(x) = \mathbb{E}_{\theta} D_G(\tilde{\eta} \parallel \eta_{\theta}).$$

259 This has similar structure to Reverse Bregman Information (RBI). Again, the deviation here
 260 is computed from another ‘‘central prediction’’.

261 One advantage of Bayesian models over point predictors is that they can give different predictions for
 262 the same input. This means we don't have to average out uncertainty; instead, we can look at the
 263 disagreements between different versions of the model. From this perspective, EPDB is especially
 264 promising because it doesn't rely on averaging but considers all possible pairwise disagreements
 265 between models, therefore it does not average out uncertainty.

266 We observe that the general approach presented in this work allows us to obtain many existing
 267 uncertainty measures in the case of the Log score loss function while leading to the whole family of
 268 new measures (see Table 1). We refer to Appendix E for additional discussion and to Appendix F for
 269 the discussion of connections of these approximations between each other. The limitations of the
 approach are discussed in detail in Appendix B.

270 4.1 BEST RISK APPROXIMATION CHOICE

271
272 Given the plethora of measures, one may fairly ask if there is a best risk approximation of each type.
273 For Excess and Total risks, we elaborate on it in Appendix E. Here, we address the choice for Bayes
274 risk.

275 Recall, that for the estimation of Bayes risk we have three options. However, it is not clear, which
276 of these approximations is better. To investigate it, we assume that there exists a vector of true
277 parameters θ^* , that for any input point x the following holds: $\eta(x) = p(y | x) = p(y | x, \theta^*)$. Note,
278 that according to equation (4), Bayes risk is concave. Using $r(\cdot) = -\mathbb{E}_x G(\cdot)$, the following follows
279 from Jensen’s inequality:

$$280 \mathbb{E}_\theta r(\eta_\theta) \leq r(\mathbb{E}_\theta \eta_\theta).$$

281 At the same time, we know that for Bayes risk the following must hold for any θ :

$$282 r(\eta) = r(p(y | x, \theta^*)) \leq r(\eta_\theta).$$

283 Hence, the following holds: $r(\eta) \leq \mathbb{E}_\theta r(\eta_\theta)$. Therefore, we have the following relation:

$$284 r(\eta) \leq \mathbb{E}_\theta r(\eta_\theta) \leq r(\mathbb{E}_\theta \eta_\theta), \quad (6)$$

285 or in other words that $R_{\text{Bayes}}^{(1)}(x)$ is tighter approximation (on average), than $R_{\text{Bayes}}^{(2)}(x)$. However, there
286 is seemingly no general answer for $r(\bar{\eta})$.

290 4.2 CONNECTION TO ENERGY-BASED MODELS

291
292 Interestingly, we can establish a connection of our framework and energy-based models (Liu et al.,
293 2020b). Let us consider a specific instantiation of MRBI for Logscore. Also, let us recap the free
294 energy function $E(x; f_\theta)$ from (Liu et al., 2020b; Grathwohl et al., 2019):

$$295 E(x; f_\theta) = -T \log \sum_{j=1}^K \exp \left[\frac{f_\theta(x)}{T} \right]_j.$$

296 It can be shown (see Section G) that

$$297 \tilde{R}_{\text{Exc}}^{(3,1)}(x) = \frac{1}{T} (E(x; \mathbb{E}_\theta f_\theta) - \mathbb{E}_\theta E(x; f_\theta)). \quad (7)$$

298 From this decomposition we see, that $\tilde{R}_{\text{Exc}}^{(3,1)}$ is the difference between two different Bayesian estimates
299 of the energy, where the first term is the energy, induced by expected logit, while second is expected
300 energy, induced by each individual set of parameters. Therefore, it is interesting to check, whether
301 $\tilde{R}_{\text{Exc}}^{(3,1)}$, predicted by our framework, will be better, than either of its components.

308 5 RELATED WORK

309
310 The field of uncertainty quantification for predictive models, especially neural networks, has seen rapid
311 advancements in recent years. Among these, methods allowing explicit uncertainty disentanglement
312 are particularly interesting due to the ability to use estimates of different sources of uncertainty in
313 various downstream tasks. For instance, epistemic uncertainty is effective in out-of-distribution data
314 detection (Hüllermeier & Waegeman, 2021; Kotelevskii et al., 2024; Mukhoti et al., 2021) and active
315 learning (Beluch et al., 2018; Gal et al., 2017).

316 Another direction in uncertainty quantification involves credal set-based approaches, which represent
317 uncertainty using sets of probability distributions. Caprio et al. (2023) introduced Credal Bayesian
318 Deep Learning, leveraging credal sets for more conservative uncertainty estimates, while Caprio
319 et al. (2024) proposed a novel Bayes’ theorem for upper probabilities. These methods offer robust
320 uncertainty quantification but can be computationally intensive, limiting their scalability.

321 Bayesian methods have become popular because they naturally handle distributions of model param-
322 eters, leading to prediction uncertainty. Exact Bayesian inference is very computationally expen-
323 sive (Izmailov et al., 2021), so many lightweight versions are used in practice (Gal & Ghahramani,
2016; Thin et al., 2021; 2020; Blei et al., 2017; Lakshminarayanan et al., 2017). Early approaches

Table 2: AUROC for different choices of function G for out-of-distribution detection with CIFAR10 as in-distribution. We used 5 groups of ensembles of size 4. We see, that in most cases, uncertainty measures, based on Log Score, appear to be better. See more detailed results in Section J.

		CIFAR100	SVHN	TinyImageNet	CIFAR10C-1	CIFAR10C-2	CIFAR10C-3	CIFAR10C-4	CIFAR10C-5
Log	$\tilde{R}_{\text{Bayes}}^{(1)}$	91.36 ± 0.05	96.01 ± 0.39	90.84 ± 0.04	60.96 ± 0.09	67.84 ± 0.09	72.59 ± 0.08	77.31 ± 0.08	83.48 ± 0.13
	$\tilde{R}_{\text{Exc}}^{(1,1)}$	90.17 ± 0.06	94.08 ± 1.02	89.32 ± 0.07	61.07 ± 0.11	67.82 ± 0.09	72.49 ± 0.08	77.15 ± 0.13	83.0 ± 0.2
	$\tilde{R}_{\text{Exc}}^{(1,2)}$	90.38 ± 0.08	94.35 ± 0.94	89.57 ± 0.07	61.1 ± 0.11	67.87 ± 0.09	72.55 ± 0.09	77.23 ± 0.13	83.14 ± 0.2
	$\tilde{R}_{\text{Exc}}^{(3,1)}$	90.38 ± 0.06	94.31 ± 0.91	89.54 ± 0.06	61.09 ± 0.11	67.86 ± 0.09	72.54 ± 0.09	77.22 ± 0.13	83.11 ± 0.19
Brier	$\tilde{R}_{\text{Bayes}}^{(1)}$	90.44 ± 0.17	96.09 ± 0.52	89.89 ± 0.13	61.03 ± 0.12	68.04 ± 0.16	72.46 ± 0.18	76.83 ± 0.18	82.47 ± 0.1
	$\tilde{R}_{\text{Exc}}^{(1,1)}$	89.24 ± 0.19	94.19 ± 0.49	88.37 ± 0.12	60.11 ± 0.15	66.59 ± 0.24	71.19 ± 0.3	75.7 ± 0.22	81.52 ± 0.16
	$\tilde{R}_{\text{Exc}}^{(1,2)}$	89.24 ± 0.19	94.19 ± 0.49	88.37 ± 0.12	60.11 ± 0.15	66.59 ± 0.24	71.19 ± 0.3	75.7 ± 0.22	81.52 ± 0.16
	$\tilde{R}_{\text{Exc}}^{(3,1)}$	89.24 ± 0.19	94.19 ± 0.49	88.37 ± 0.12	60.11 ± 0.15	66.59 ± 0.24	71.19 ± 0.3	75.7 ± 0.22	81.52 ± 0.16
Spherical	$\tilde{R}_{\text{Bayes}}^{(1)}$	90.46 ± 0.04	96.15 ± 0.4	89.95 ± 0.19	61.47 ± 0.19	68.54 ± 0.23	72.95 ± 0.28	77.39 ± 0.34	82.99 ± 0.43
	$\tilde{R}_{\text{Exc}}^{(1,1)}$	89.11 ± 0.15	93.77 ± 0.66	88.28 ± 0.2	60.54 ± 0.18	66.88 ± 0.26	71.36 ± 0.29	75.96 ± 0.29	81.89 ± 0.33
	$\tilde{R}_{\text{Exc}}^{(1,2)}$	89.17 ± 0.14	93.86 ± 0.66	88.35 ± 0.2	60.54 ± 0.18	66.88 ± 0.26	71.37 ± 0.3	75.97 ± 0.29	81.91 ± 0.34
	$\tilde{R}_{\text{Exc}}^{(3,1)}$	89.1 ± 0.15	93.78 ± 0.66	88.27 ± 0.2	60.54 ± 0.18	66.88 ± 0.26	71.35 ± 0.29	75.95 ± 0.29	81.88 ± 0.33

inspired by Bayesian ideas (Gal et al., 2017; Kendall & Gal, 2017; Lakshminarayanan et al., 2017) used information-based measures like Mutual Information (Houlsby et al., 2011; Malinin & Gales, 2021) to quantify epistemic uncertainty and measures like entropy or maximum probability for aleatoric uncertainty. These methods, despite different computational costs, are widely used in the field.

However, the practical expense of Bayesian inference, even in its approximate forms, has led to the introduction of more simplified approaches. Some of these methods leverage hidden neural network representations, considering distances in their hidden space as a proxy for epistemic uncertainty estimation (Van Amersfoort et al., 2020; Liu et al., 2020a; Kotelevskii et al., 2022; Mukhoti et al., 2021). While they offer the advantage of requiring only a single pass over the network, their notion of epistemic uncertainty, often linked to the distance of an object’s representation to training data, captures only a part of the full epistemic uncertainty. Despite this limitation, their efficiency and effectiveness in out-of-distribution detection have made them widely used. [Another class of models for uncertainty quantification that utilizes generative models \(e.g., diffusion models or normalizing flows\) has been recently explored \(Berry & Meger, 2023; Chan et al., 2024\). While these methods offer a promising direction, they require training a generative model, which can be computationally intensive and may limit their applicability in certain settings.](#)

Works by Gruber & Buettner (2023); Adlam et al. (2022) are close to us. In both papers, decompositions of Bregman divergence loss functions are discussed. While the main focus of these papers is generalized bias-variance decomposition, Gruber & Buettner (2023) also considers an application to uncertainty quantification. In terms of our framework, they arrive to the following decomposition (see derivation in Appendix F):

$$\tilde{R}_{\text{Tot}}^{(1,1)} = \tilde{R}_{\text{Bayes}}^{(2)} + \tilde{R}_{\text{Exc}}^{(3,1)} + \tilde{R}_{\text{Exc}}^{(2,3)}, \quad (8)$$

which is only a partial case of our framework. There, they called $\tilde{R}_{\text{Exc}}^{(3,1)}$ as generalized “variance”, and use it as a measure of uncertainty for out-of-distribution detection. However, it is not clear, why exactly this decomposition and approximations were chosen. For example, as we showed in Section 4.1, $\tilde{R}_{\text{Bayes}}^{(1)}$ leads to a tighter approximation of Bayes risk on average, than $\tilde{R}_{\text{Bayes}}^{(2)}$.

[Works by Kotelevskii et al. \(2022\), Lahlou et al. \(2023\), and Liu et al. \(2019\) also consider the same decomposition of risks. However, in all these papers, only specific approximations were explored, and no general connection among existing measures was established.](#)

Despite the diversity of these approaches, the arbitrary nature of choosing uncertainty measures has led to ambiguity in understanding uncertainty. This paper aims to address this gap by proposing a unified framework that not only categorizes these diverse methods but also offers a more comprehensive understanding of uncertainty quantification.

6 EXPERIMENTS

In this section, we test different uncertainty measures derived from our general framework. Any Bayesian method that produces multiple samples of model weights (or parameters of the first-order distribution) can be used to compute our proposed measures. However, deep ensembles are considered the “gold standard” in uncertainty quantification (Lakshminarayanan et al., 2017). Therefore, for our experiments, we use deep ensembles trained with various strictly proper scoring rules as loss functions. As training (in-distribution) datasets, we consider CIFAR10, CIFAR100 (Krizhevsky et al., 2009), and TinyImageNet.

We evaluate the proposed measures of uncertainty by focusing on two specific problems: *out-of-distribution detection* and *misclassification detection*. For both problems, we trained five deep ensembles independently, each consisting of four members—resulting in a total of 20 models trained completely independently. All ensemble members shared the same architecture but differed due to randomness in initialization and training. We used ResNet18 (He et al., 2016) as the architecture (additional details can be found in Appendix H). Note that in all the tables below, we report the average performance across different groups of ensembles (AUROC), along with the corresponding standard deviation.

Our experimental evaluation aims to answer the following questions:

1. Is there a best function G that yields better results in the considered downstream tasks?
2. Is Excess risk always better than Bayes risk for out-of-distribution detection?
3. Is Total risk always better than Excess risk for misclassification detection?
4. Is the measure of uncertainty proposed by our framework better than other Bayesian estimates of the energy?

We emphasize that the goal of our experimental evaluation is *not to provide new state-of-the-art measures or compete with other known approaches* for uncertainty quantification. Instead, we aim to *verify whether different uncertainty estimates are indeed related to specific types of uncertainty*. We refer readers to Appendix A, where we discuss why one might expect either type of uncertainty to be good for a specific task. Additionally, we refer the reader to Appendix M for a specific toy example where our measures of epistemic uncertainty can be computed in closed form. In this example, we also discuss cases of prior misspecification and model misspecification.

6.1 IS THERE A BEST FUNCTION PLUG-IN CHOICE?

In this section, we address the first question. For this, we consider some specific risks and different plug-in choices for the function G . As a loss function, we use strictly proper scoring rules generated by the same function G (hence, we do not include the Zero-One score, as it is not differentiable). We present results in Table 2 (see additional results in Tables 5, 6, 7, 8 and 9). We see that, in most cases, the Log Score performs better than the others. This result is reassuring because Log Score-based measures are the popular choice in the literature on uncertainty quantification. As for misclassification detection (see Tables 4, 10, 11, 12, and 13), the results are more comparable, but Log Score is still a good choice.

Hence, the answer to the first question is the following: there is no all-time-best plug-in choice of G . However, Log Score-based measures (that are already popular in practice) are typically a good choice in the considered downstream tasks.

6.2 IS EXCESS RISK BETTER THAN BAYES RISK FOR OUT-OF-DISTRIBUTION DETECTION?

In this section, we evaluate different instances of our framework to identify out-of-distribution samples. Since the uncertainty associated with OOD detection is of epistemic nature (see Appendix A for discussion), we expect that Excess and Total risks will perform well for this task, while Bayes risk will likely fail. In the main part, we consider two datasets as in-distribution, namely CIFAR10 in Table 2 and TinyImageNet in Table 3. For more experiments, we refer to Appendix J.

We distinguish between two types of out-of-distribution data: “soft-OOD” and “hard-OOD”. Both are special cases of covariate shift. “Soft-OOD” samples, such as slightly changed versions of CIFAR10

Table 3: AUROC (Log Score) for OOD detection with TinyImageNet in-distribution.

	ImageNet-A	ImageNet-R	ImageNet-O
$\tilde{R}_{\text{Bayes}}^{(1)}$	83.22 ± 0.24	82.23 ± 0.39	72.21 ± 0.22
$\tilde{R}_{\text{Bayes}}^{(2)}$	83.76 ± 0.24	82.78 ± 0.37	73.18 ± 0.2
$\tilde{R}_{\text{Bayes}}^{(3)}$	83.61 ± 0.2	82.67 ± 0.37	72.86 ± 0.3
$\tilde{R}_{\text{Exc}}^{(1,1)}$	77.11 ± 0.34	76.52 ± 0.19	74.46 ± 0.18
$\tilde{R}_{\text{Exc}}^{(1,2)}$	79.09 ± 0.33	78.38 ± 0.17	74.79 ± 0.25
$\tilde{R}_{\text{Exc}}^{(2,1)}$	75.94 ± 0.36	75.4 ± 0.23	74.07 ± 0.18
$\tilde{R}_{\text{Exc}}^{(1,3)}$	76.21 ± 0.43	75.55 ± 0.21	73.84 ± 0.17
$\tilde{R}_{\text{Exc}}^{(3,1)}$	77.56 ± 0.28	77.02 ± 0.17	74.46 ± 0.22
$\tilde{R}_{\text{Tot}}^{(1,1)}$	84.26 ± 0.23	83.32 ± 0.31	74.93 ± 0.17
$\tilde{R}_{\text{Tot}}^{(1,2)}$	83.76 ± 0.24	82.78 ± 0.37	73.18 ± 0.2
$\tilde{R}_{\text{Tot}}^{(1,3)}$	83.93 ± 0.24	82.95 ± 0.36	73.72 ± 0.16
$\tilde{R}_{\text{Tot}}^{(3,1)}$	83.88 ± 0.19	82.99 ± 0.32	74.09 ± 0.27
$E(x; \mathbb{E}_\theta f_\theta)$	83.96 ± 0.23	83.28 ± 0.41	72.72 ± 0.33
$\mathbb{E}_\theta E(x; f_\theta)$	82.99 ± 0.26	82.31 ± 0.45	71.15 ± 0.34

Table 4: AUROC (Log Score) for misclassification detection. For loss function and uncertainty plug-in, we use the same G , that corresponds to Log Score. CIFAR10-N and CIFAR100-N stand for noisy versions of these datasets (see Section I).

	CIFAR10	CIFAR100	CIFAR10-N	CIFAR100-N	TinyImageNet
$\tilde{R}_{\text{Bayes}}^{(1)}$	94.39 ± 0.08	84.61 ± 0.35	78.26 ± 4.11	81.9 ± 0.29	84.99 ± 0.24
$\tilde{R}_{\text{Bayes}}^{(2)}$	94.7 ± 0.05	85.13 ± 0.35	78.36 ± 4.77	81.92 ± 0.36	85.5 ± 0.23
$\tilde{R}_{\text{Bayes}}^{(3)}$	94.76 ± 0.09	85.95 ± 0.31	80.44 ± 3.69	83.41 ± 0.23	86.55 ± 0.26
$\tilde{R}_{\text{Exc}}^{(1,1)}$	94.1 ± 0.14	81.58 ± 0.34	68.39 ± 6.07	74.52 ± 0.83	81.33 ± 0.29
$\tilde{R}_{\text{Exc}}^{(1,2)}$	94.23 ± 0.14	82.9 ± 0.31	69.64 ± 6.1	75.74 ± 0.78	83.22 ± 0.28
$\tilde{R}_{\text{Exc}}^{(2,1)}$	94.01 ± 0.14	80.69 ± 0.35	67.7 ± 6.09	73.7 ± 0.86	80.18 ± 0.31
$\tilde{R}_{\text{Exc}}^{(1,3)}$	93.72 ± 0.16	80.3 ± 0.33	66.85 ± 5.94	73.37 ± 0.87	79.25 ± 0.25
$\tilde{R}_{\text{Exc}}^{(3,1)}$	94.4 ± 0.13	82.62 ± 0.34	69.98 ± 6.08	75.51 ± 0.8	82.74 ± 0.34
$\tilde{R}_{\text{Tot}}^{(1,1)}$	94.5 ± 0.06	85.43 ± 0.35	75.73 ± 4.68	81.67 ± 0.41	85.58 ± 0.22
$\tilde{R}_{\text{Tot}}^{(1,2)}$	94.7 ± 0.05	85.13 ± 0.35	78.36 ± 4.77	81.92 ± 0.36	85.5 ± 0.23
$\tilde{R}_{\text{Tot}}^{(1,3)}$	94.4 ± 0.06	85.01 ± 0.37	76.26 ± 5.04	81.67 ± 0.39	85.18 ± 0.23
$\tilde{R}_{\text{Tot}}^{(3,1)}$	94.74 ± 0.07	86.22 ± 0.31	79.38 ± 3.85	83.18 ± 0.29	86.65 ± 0.26

or TinyImageNet, have predicted probability vectors that are still meaningful (see discussion in Appendix B). In our experiments, CIFAR10C can be considered as “soft-OOD”, as it is a corrupted version of CIFAR10, while ImageNet-O (see description in Appendix I) is “soft-OOD” for TinyImageNet. “Hard-OOD” samples, however, have completely non-informative predicted probability vectors. For example, when a set of classes is considered during training, but an incoming image does not belong to those classes, the resulting probability distribution over training classes is meaningless.

From the Tables 2 and 3, we see that Excess risk is a good choice for “soft-OOD” (especially in case of Log score). However, as data become more “hard-OOD”, the results are unexpected – Bayes risk typically outperforms Excess risk. We provide one possible explanation of this effect in Appendix A.

This highlights a **crucial limitation of Excess risk (which includes ubiquitous BI, RBI, and EPBD) as a measure of epistemic uncertainty**. These measures naturally appear when approximating Excess risk in a Bayesian way, which assumes a specific form of ground-truth distribution approximation. However, this approximation becomes inaccurate for “hard-OOD” samples, making these measures a poor choice in these cases. This criticism aligns with findings from (Wimmer et al., 2023; Schweighofer et al., 2023a; Bengs et al., 2023), which indicate that Bregman Information (in a particular case of Log score) is not an intuitive measure of epistemic uncertainty and does not follow their proposed axioms.

Therefore, the answer to the second question is not absolute. For “soft-OOD” samples, where predicted probability vectors remain meaningful, Excess risk is a good choice. For “hard-OOD” samples, Bayes risk is typically better. Total risk consistently shows decent results, making it a safe choice when the nature of incoming data is unknown.

6.3 IS TOTAL RISK ALWAYS BETTER THAN EXCESS RISK FOR MISCLASSIFICATION DETECTION?

We now consider misclassification detection. Misclassification detection is intuitively connected to aleatoric and total uncertainties (see Appendix A). Therefore, we expect Bayes and Total risks to perform well in this task, while all instances of Excess risk should perform **typically worse (given the scenario that there is enough training (in-distribution) data)**.

It is known that standard versions of CIFAR10 and CIFAR100 lack significant aleatoric uncertainty (Kapoor et al., 2022), making it challenging to demonstrate the usefulness of the appropriate uncertainty measures immediately. To address this, we create special versions of these datasets with introduced label noise (see details in Appendix I).

From the Table 4 we see that Bayes and Total risks indeed outperform Excess risk for misclassification detection (see additional results in Appendix K). Moreover, the difference in performance becomes more significant as more aleatoric noise is introduced into the training dataset. Hence, the answer to this question is mostly positive. Bayes risk and Total risk are better for misclassification detection.

6.4 WHICH ENERGY ESTIMATE IS BETTER?

We discovered a connection between our approach and energy-based models that are used for out-of-distribution detection. However, in our approach, energy appears as the difference between two different Bayesian energy estimates for a particular choice of G . Which one of these three quantities, based on energy, is better?

Based on the results in Table 3 (and in Tables 5, 9, 10 and 13 in Appendix) we can conclude, that $E(x; \mathbb{E}_\theta f_\theta)$ is consistently better, than $\mathbb{E}_\theta E(x; f_\theta)$ in both considered problems. Specifically, $\tilde{R}_{\text{Exc}}^{(3,1)}$ performs better than both energy estimates for misclassification detection on all the datasets in Table 10, while for TinyImageNet the results are close (see Table 13). $\tilde{R}_{\text{Exc}}^{(3,1)}$ is also preferred over energy estimates for Soft-OOD detection for ImageNet-O (see Tables 3 and Table 9) and CIFAR10C[1,2] (see Table 5).

When the out-of-distribution detection problem is considered and “hard-OOD” is encountered, $\tilde{R}_{\text{Exc}}^{(3,1)}$ is typically worse than both of the energy estimates in terms of AUROC. However, when “soft-OOD” is encountered, their difference $\tilde{R}_{\text{Exc}}^{(3,1)}$, as a particular instance of Excess risk, becomes more effective than both of them (see results on ImageNet-O and extended Table 9). When the misclassification detection problem is considered, $\tilde{R}_{\text{Exc}}^{(3,1)}$ is better than both of the estimates.

Hence, the answer is in line with what we discussed above: Excess risk (and in particular $\tilde{R}_{\text{Exc}}^{(3,1)}$) is a good choice for “soft-OOD.” Therefore, when this is the case, $\tilde{R}_{\text{Exc}}^{(3,1)}$ performs well. When “hard-OOD” is the case, $E(x; \mathbb{E}_\theta f_\theta)$ is typically better.

7 CONCLUSION

In this paper, we developed a general framework for predictive uncertainty estimation using pointwise risk estimation and strictly proper scoring rules as loss functions. We proposed pointwise risk as a natural measure of predictive uncertainty and derived general results for total, epistemic, and aleatoric uncertainties, demonstrating that epistemic uncertainties can be represented as a Bregman divergence within this framework.

We incorporated Bayesian reasoning into our framework, showing that commonly used measures of epistemic uncertainty, such as Mutual Information and Expected Pairwise Kullback-Leibler divergence, are special cases within our general approach. We also discussed the limitations of our framework, elaborating on recent critiques in the literature (Wimmer et al., 2023; Schweighofer et al., 2023a). Moreover, we showed, that even energy-based models fall into the framework, as a particular approximation of Excess risk.

Finally, in our experiments on image datasets, we evaluated these measures for out-of-distribution detection and misclassification detection tasks and discussed which measures are most suitable for each scenario.

REFERENCES

- Ben Adlam, Neha Gupta, Zeld Mariet, and Jamie Smith. Understanding the bias-variance tradeoff of bregman divergences. *arXiv preprint arXiv:2202.04167*, 2022.
- William H Beluch, Tim Genewein, Andreas Nürnberger, and Jan M Köhler. The power of ensembles for active learning in image classification. In *Proceedings of the IEEE conference on computer vision and pattern recognition*, pp. 9368–9377, 2018.
- Viktor Bengs, Eyke Hüllermeier, and Willem Waegeman. On second-order scoring rules for epistemic uncertainty quantification. In *International Conference on Machine Learning*, pp. 2078–2091. PMLR, 2023.
- Lucas Berry and David Meger. Escaping the sample trap: Fast and accurate epistemic uncertainty estimation with pairwise-distance estimators. *arXiv preprint arXiv:2308.13498*, 2023.

-
- 540 David M Blei, Alp Kucukelbir, and Jon D McAuliffe. Variational inference: A review for statisticians.
541 *Journal of the American statistical Association*, 112(518):859–877, 2017.
- 542 Lev M Bregman. The relaxation method of finding the common point of convex sets and its
543 application to the solution of problems in convex programming. *USSR computational mathematics*
544 *and mathematical physics*, 7(3):200–217, 1967.
- 546 Michele Caprio, Souradeep Dutta, Kuk Jin Jang, Vivian Lin, Radoslav Ivanov, Oleg Sokolsky, and
547 Insup Lee. Imprecise bayesian neural networks. *arXiv preprint arXiv:2302.09656*, 2023.
- 548 Michele Caprio, Yusuf Sale, Eyke Hüllermeier, and Insup Lee. A novel bayes’ theorem for upper
549 probabilities. In Fabio Cuzzolin and Maryam Sultana (eds.), *Epistemic Uncertainty in Artificial*
550 *Intelligence*, pp. 1–12, Cham, 2024. Springer Nature Switzerland. ISBN 978-3-031-57963-9.
- 552 Matthew A Chan, Maria J Molina, and Christopher A Metzler. Hyper-diffusion: Estimating epistemic
553 and aleatoric uncertainty with a single model. *arXiv preprint arXiv:2402.03478*, 2024.
- 554 Yarin Gal and Zoubin Ghahramani. Dropout as a bayesian approximation: Representing model
555 uncertainty in deep learning. In *international conference on machine learning*, pp. 1050–1059.
556 PMLR, 2016.
- 557 Yarin Gal, Riashat Islam, and Zoubin Ghahramani. Deep bayesian active learning with image data.
558 In *International conference on machine learning*, pp. 1183–1192. PMLR, 2017.
- 560 Yonatan Geifman and Ran El-Yaniv. Selective classification for deep neural networks. *Advances in*
561 *neural information processing systems*, 30, 2017.
- 562 Tilmann Gneiting and Adrian E Raftery. Strictly proper scoring rules, prediction, and estimation.
563 *Journal of the American statistical Association*, 102(477):359–378, 2007.
- 564 Will Grathwohl, Kuan-Chieh Wang, Jörn-Henrik Jacobsen, David Duvenaud, Mohammad Norouzi,
565 and Kevin Swersky. Your classifier is secretly an energy based model and you should treat it like
566 one. *arXiv preprint arXiv:1912.03263*, 2019.
- 568 Sorin Grigorescu, Bogdan Trasnea, Tiberiu Cocias, and Gigel Macesanu. A survey of deep learning
569 techniques for autonomous driving. *Journal of Field Robotics*, 37(3):362–386, 2020.
- 570 Sebastian Gruber and Florian Buettner. Uncertainty estimates of predictions via a general bias-
571 variance decomposition. In *International Conference on Artificial Intelligence and Statistics*, pp.
572 11331–11354. PMLR, 2023.
- 574 Kaiming He, Xiangyu Zhang, Shaoqing Ren, and Jian Sun. Deep residual learning for image
575 recognition. In *Proceedings of the IEEE conference on computer vision and pattern recognition*,
576 pp. 770–778, 2016.
- 577 James B Heaton, Nick G Polson, and Jan Hendrik Witte. Deep learning for finance: deep portfolios.
578 *Applied Stochastic Models in Business and Industry*, 33(1):3–12, 2017.
- 580 Dan Hendrycks, Steven Basart, Norman Mu, Saurav Kadavath, Frank Wang, Evan Dorundo, Rahul
581 Desai, Tyler Zhu, Samyak Parajuli, Mike Guo, Dawn Song, Jacob Steinhardt, and Justin Gilmer.
582 The many faces of robustness: A critical analysis of out-of-distribution generalization. *ICCV*,
583 2021a.
- 584 Dan Hendrycks, Kevin Zhao, Steven Basart, Jacob Steinhardt, and Dawn Song. Natural adversarial
585 examples. *CVPR*, 2021b.
- 586 Neil Houlsby, Ferenc Huszár, Zoubin Ghahramani, and Máté Lengyel. Bayesian active learning for
587 classification and preference learning. *arXiv preprint arXiv:1112.5745*, 2011.
- 588 Eyke Hüllermeier and Willem Waegeman. Aleatoric and epistemic uncertainty in machine learning:
589 An introduction to concepts and methods. *Machine Learning*, 110:457–506, 2021.
- 590 Pavel Izmailov, Sharad Vikram, Matthew D Hoffman, and Andrew Gordon Gordon Wilson. What are
591 bayesian neural network posteriors really like? In *International conference on machine learning*,
592 pp. 4629–4640. PMLR, 2021.
- 593

-
- 594 Sanyam Kapoor, Wesley J Maddox, Pavel Izmailov, and Andrew G Wilson. On uncertainty, tempering,
595 and data augmentation in bayesian classification. *Advances in Neural Information Processing*
596 *Systems*, 35:18211–18225, 2022.
- 597
- 598 Alex Kendall and Yarin Gal. What uncertainties do we need in bayesian deep learning for computer
599 vision? *Advances in neural information processing systems*, 30, 2017.
- 600
- 601 Nikita Kotelevskii, Aleksandr Artemenkov, Kirill Fedyanin, Fedor Noskov, Alexander Fishkov,
602 Artem Shelmanov, Artem Vazhentsev, Aleksandr Petiushko, and Maxim Panov. Nonparametric
603 uncertainty quantification for single deterministic neural network. *Advances in Neural Information*
604 *Processing Systems*, 35:36308–36323, 2022.
- 605
- 606 Nikita Kotelevskii, Samuel Horváth, Karthik Nandakumar, Martin Takac, and Maxim Panov. Dirichlet-
607 based uncertainty quantification for personalized federated learning with improved posterior
608 networks. In Kate Larson (ed.), *Proceedings of the Thirty-Third International Joint Conference*
609 *on Artificial Intelligence, IJCAI-24*, pp. 7127–7135. International Joint Conferences on Artificial
610 Intelligence Organization, 8 2024. doi: 10.24963/ijcai.2024/788. URL <https://doi.org/10.24963/ijcai.2024/788>. Main Track.
- 611
- 612 Alex Krizhevsky, Geoffrey Hinton, et al. Learning multiple layers of features from tiny images. 2009.
- 613
- 614 Salem Lahlou, Moksh Jain, Hadi Nekoei, Victor I Butoi, Paul Bertin, Jarrid Rector-Brooks, Maksym
615 Korablyov, and Yoshua Bengio. Deup: Direct epistemic uncertainty prediction. *Transactions on*
Machine Learning Research, 2023.
- 616
- 617 Balaji Lakshminarayanan, Alexander Pritzel, and Charles Blundell. Simple and scalable predictive
618 uncertainty estimation using deep ensembles. *Advances in neural information processing systems*,
619 30, 2017.
- 620
- 621 Geert Litjens, Thijs Kooi, Babak Ehteshami Bejnordi, Arnaud Arindra Adiyoso Setio, Francesco
622 Ciompi, Mohsen Ghafoorian, Jeroen Awm Van Der Laak, Bram Van Ginneken, and Clara I Sánchez.
A survey on deep learning in medical image analysis. *Medical image analysis*, 42:60–88, 2017.
- 623
- 624 Jeremiah Liu, John Paisley, Marianthi-Anna Kioumourtoglou, and Brent Coull. Accurate uncertainty
625 estimation and decomposition in ensemble learning. *Advances in neural information processing*
626 *systems*, 32, 2019.
- 627
- 628 Jeremiah Liu, Zi Lin, Shreyas Padhy, Dustin Tran, Tania Bedrax Weiss, and Balaji Lakshminarayanan.
Simple and principled uncertainty estimation with deterministic deep learning via distance aware-
629 ness. *Advances in Neural Information Processing Systems*, 33:7498–7512, 2020a.
- 630
- 631 Weitang Liu, Xiaoyun Wang, John Owens, and Yixuan Li. Energy-based out-of-distribution detection.
632 *Advances in neural information processing systems*, 33:21464–21475, 2020b.
- 633
- 634 Andrey Malinin and Mark Gales. Predictive uncertainty estimation via prior networks. *Advances in*
neural information processing systems, 31, 2018.
- 635
- 636 Andrey Malinin and Mark Gales. Uncertainty estimation in autoregressive structured prediction. *In*
637 *International Conference on Learning Representations.*, 2021.
- 638
- 639 Sajjad Mozaffari, Omar Y Al-Jarrah, Mehrdad Dianati, Paul Jennings, and Alexandros Mouzakitis.
Deep learning-based vehicle behavior prediction for autonomous driving applications: A review.
640 *IEEE Transactions on Intelligent Transportation Systems*, 23(1):33–47, 2020.
- 641
- 642 Jishnu Mukhoti, Joost van Amersfoort, Philip HS Torr, and Yarin Gal. Deep deterministic uncertainty
643 for semantic segmentation. *arXiv preprint arXiv:2111.00079*, 2021.
- 644
- 645 Ahmet Murat Ozbayoglu, Mehmet Ugur Gudelek, and Omer Berat Sezer. Deep learning for financial
646 applications: A survey. *Applied Soft Computing*, 93:106384, 2020.
- 647
- David Pfau. A generalized bias-variance decomposition for bregman divergences. 2013. URL
http://www.daviddpfau.com/assets/generalized_bvd_proof.pdf.

648 Kajetan Schweighofer, Lukas Aichberger, Mykyta Ielanskyi, and Sepp Hochreiter. Introducing an
649 improved information-theoretic measure of predictive uncertainty. In *NeurIPS 2023 Workshop on*
650 *Mathematics of Modern Machine Learning*, 2023a.

651
652 Kajetan Schweighofer, Lukas Aichberger, Mykyta Ielanskyi, Günter Klambauer, and Sepp
653 Hochreiter. Quantification of uncertainty with adversarial models. In A. Oh, T. Nau-
654 mann, A. Globerson, K. Saenko, M. Hardt, and S. Levine (eds.), *Advances in Neural*
655 *Information Processing Systems*, volume 36, pp. 19446–19484. Curran Associates, Inc.,
656 2023b. URL [https://proceedings.neurips.cc/paper_files/paper/2023/](https://proceedings.neurips.cc/paper_files/paper/2023/file/3e0b96206965f5f05b0b4550c0e73ff0-Paper-Conference.pdf)
657 [file/3e0b96206965f5f05b0b4550c0e73ff0-Paper-Conference.pdf](https://proceedings.neurips.cc/paper_files/paper/2023/file/3e0b96206965f5f05b0b4550c0e73ff0-Paper-Conference.pdf).

658 Dinggang Shen, Guorong Wu, and Heung-II Suk. Deep learning in medical image analysis. *Annual*
659 *review of biomedical engineering*, 19:221–248, 2017.

660
661 Achille Thin, Nikita Kotelevskii, Jean-Stanislas Denain, Leo Grinsztajn, Alain Durmus, Maxim
662 Panov, and Eric Moulines. Metflow: a new efficient method for bridging the gap between markov
663 chain monte carlo and variational inference. *arXiv preprint arXiv:2002.12253*, 2020.

664 Achille Thin, Nikita Kotelevskii, Arnaud Doucet, Alain Durmus, Eric Moulines, and Maxim Panov.
665 Monte carlo variational auto-encoders. In *International Conference on Machine Learning*, pp.
666 10247–10257. PMLR, 2021.

667
668 Joost Van Amersfoort, Lewis Smith, Yee Whye Teh, and Yarin Gal. Uncertainty estimation using a
669 single deep deterministic neural network. In *International conference on machine learning*, pp.
670 9690–9700. PMLR, 2020.

671
672 Lisa Wimmer, Yusuf Sale, Paul Hofman, Bernd Bischl, and Eyke Hüllermeier. Quantifying aleatoric
673 and epistemic uncertainty in machine learning: Are conditional entropy and mutual information
674 appropriate measures? In *Uncertainty in Artificial Intelligence*, pp. 2282–2292. PMLR, 2023.

675
676
677
678
679
680
681
682
683
684
685
686
687
688
689
690
691
692
693
694
695
696
697
698
699
700
701

A WHY IS EPISTEMIC UNCERTAINTY GOOD FOR OUT-OF-DISTRIBUTION DETECTION, AND TOTAL FOR MISCLASSIFICATION DETECTION?

Generally speaking, the out-of-distribution detection problem is not directly related to the conditional distribution $p(y | x)$, which is at the core of our paper and generally of supervised learning. The formally correct approach would be to consider some approximation of the covariate distribution $p(x)$ and perform out-of-distribution detection based on it.

However, in the literature, both aleatoric uncertainty (related solely to $p(y | x)$) and epistemic uncertainty (associated with the quality of estimation for $p(y | x)$) are applied to solve the out-of-distribution problem and demonstrate certain performance in the task.

The success of aleatoric uncertainty that we observe in our experiments for “hard-OOD”, might seem mysterious as, conceptually, it is not related to the covariate distribution at all. The empirical success of aleatoric uncertainty for detecting out-of-distribution is related to the fact that the models are usually overconfident for in-distribution objects, leading to very low uncertainty. At the same time, the model confidence for out-of-distribution samples is more arbitrary as nothing pushes the model to be confident in them. Thus, out-of-distribution samples may have higher aleatoric uncertainty than in-distribution objects.

At the same time, the application of epistemic uncertainty to out-of-distribution detection is more grounded, as one can expect that we have less knowledge about the actual dependence for out-of-distribution objects than we do for in-distribution objects. This relation can be formalized for some models, such as kernel methods. For example, the work by Kotelevskii et al. (2022) shows that $p(x)$ epistemic uncertainty is proportional to the inverse of for Nadaraya-Watson kernel regression. Moreover, this method falls into the same risk decomposition, but is built on another approximation.

For the Bayesian approximations we considered (except constant approximations), Excess risk can be seen as a “measure of disagreement” between predictions of the members of the ensemble. One may expect ensemble members to have arbitrarily different and diverse predictions for out-of-distribution data, resulting in higher values of Excess risk. Lots of literature on the topic has the same flavor of reasoning. For example, uncertainty papers about Mutual Information, EPKL (Malinin & Gales, 2021; Lakshminarayanan et al., 2017; Gal et al., 2017; Schweighofer et al., 2023a), etc., are the particular case of our framework.

Similarly, total and aleatoric uncertainty measures are effective for misclassification detection because they capture the inherent ambiguity or noise in the data associated with specific inputs. Aleatoric uncertainty reflects the variability in the model’s predictions due to the inherent randomness or non-deterministic dependency between covariates and labels, which is a common source of misclassification. Therefore, when a model encounters an input that is difficult to map to a certain class, the aleatoric uncertainty increases.

Measures of epistemic uncertainty effectively capture the disagreement between different members or samples of a Bayesian model. Hence, if there is a non-deterministic dependency between covariates and labels, epistemic uncertainty might increase as well, as different models may produce varying predictions for the same input. Therefore, the sum of both uncertainties—namely, total uncertainty—should be the most effective measure for detecting misclassification events.

B LIMITATIONS

We see two limitations to our approach.

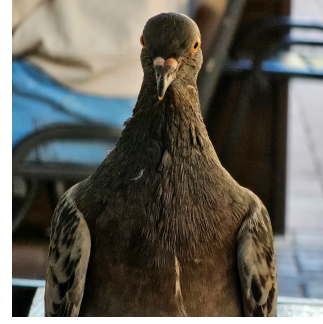
Valid conditional $\eta(x) = p(y | x)$ for all x . This assumption implies, that regardless of the input x , the form of the probability distribution $\eta(x)$ will not change. This means, that even for inputs, that do not belong to $P_{tr}(X)$, the conditional should produce some categorical vector over the same number of classes. Let us consider an example of a binary classification problem, where we want our model to distinguish between cats and dogs (see Figure 1). In this case, the distribution of covariates $P_{tr}(X)$ is the distribution over images of all possible cats and dogs. An image of a pigeon under this distribution should have a negligible probability. Now imagine, that somehow it happened that x is actually an image of a pigeon. Under our assumption, $\eta(x)$ should be valid, so it should



A dog, has sufficient probability under P_{tr} . Conditional $\eta(x)$ is **meaningful**.



A cat, has sufficient probability under P_{tr} . Conditional $\eta(x)$ is **meaningful**.



A pigeon, has almost no probability mass under P_{tr} . Conditional $\eta(x)$ is **vague**.

Figure 1: The figure shows different examples of input objects in binary classification problem (cats vs dogs). The limitation of our approach is that $\eta(x) = P_{tr}(Y | X = x)$ should be defined even for objects with tiny mass under P_{tr} (see discussion in Section B).

produce a vector of probabilities over two classes: Cats and Dogs, despite an input being an apparent out-of-distribution object. There is no good way to define $\eta(x)$ for such input objects, hence we say it is vague. However, for unusual (but still in-distribution) inputs, like rare dog breeds, $\eta(x)$ is meaningful.

Incorporation of Bayesian reasoning for estimation of η . In practice, we do not have access to $\eta(x)$. Hence, we suggested approximating it using the Bayesian approach and proposed two ideas to do it (inner and outer expectations). For Bayes risk the best Bayesian estimate is given by outer expectation (see Appendix E). However, this is not the case for Excess risk. It appears (see discussion in Appendix E) that Excess risk depends on the estimate of the Total risk. But we never know in advance for a particular input x , in which regime (overestimated or underestimated Total risk) we are. Thus, we do not know what is the best choice for an approximation to epistemic uncertainty.

C DERIVATIONS OF DIFFERENT RISKS WITH PROPER SCORING RULES

We will start with the derivation of Total risk. In what follows, we will omit dependency on x for $\eta(x)$ and $\eta_\theta(x)$.

$$\begin{aligned} R_{\text{Tot}}(\eta_\theta | x) &= \int \ell(\eta_\theta, y) dP(y | x) = \sum_{k=1}^K \left(\langle G'(\eta_\theta), \eta_\theta \rangle - G'_k(\eta_\theta) - G(\eta_\theta) \right) \eta_k = \\ & \langle G'(\eta_\theta), \eta_\theta \rangle - G(\eta_\theta) - \langle G'(\eta_\theta), \eta \rangle. \end{aligned}$$

Let us now consider Bayes risk:

$$\begin{aligned} R_{\text{Bayes}}(x) &= \int \ell(\eta, y) dP(y | x) = \sum_{k=1}^K \left(\langle G'(\eta), \eta \rangle - G'_k(\eta) - G(\eta) \right) \eta_k = \\ & \langle G'(\eta), \eta \rangle - \langle G'(\eta), \eta \rangle - G(\eta) = -G(\eta). \end{aligned}$$

Finally, let us consider Excess risk:

$$\begin{aligned} R_{\text{Exc}}(\eta_\theta | x) &= \underbrace{\int \ell(\eta_\theta, y) dP(y | x)}_{\text{Total risk}} - \underbrace{\int \ell(\eta, y) dP(y | x)}_{\text{Bayes risk}} = \\ & \langle G'(\eta_\theta), \eta_\theta \rangle - G(\eta_\theta) - \langle G'(\eta_\theta), \eta \rangle + G(\eta) = \\ & G(\eta) - G(\eta_\theta) - \langle G'(\eta_\theta), \eta - \eta_\theta \rangle := D_G(\eta || \eta_\theta). \end{aligned}$$

D DERIVATION OF RISKS FOR SPECIFIC CHOICES OF SCORING RULES

In this section, we will derive specific equations for Total, Bayes, and Excess pointwise risks to get the estimates of total, aleatoric, and epistemic uncertainties correspondingly. We will omit subscript θ in this section, indicating an estimate by using a hat.

Recall equations for proper scoring rule and different risks:

$$\begin{aligned}\ell(\eta, i) &= \langle G'(\eta), \eta \rangle - G'_i(\eta) - G(\eta), \\ \mathbf{R}_{\text{Tot}} &= \langle G'(\hat{\eta}), \hat{\eta} \rangle - G(\hat{\eta}) - \langle G'(\hat{\eta}), \eta \rangle, \\ \mathbf{R}_{\text{Bayes}} &= -G(\eta), \\ \mathbf{R}_{\text{Exc}} &= G(\eta) - G(\hat{\eta}) + \langle G'(\hat{\eta}), \hat{\eta} - \eta \rangle.\end{aligned}$$

D.1 LOG SCORE (CROSS-ENTROPY)

$$G(\eta) = \sum_{k=1}^K \eta_k \log \eta_k,$$

$$G'(\eta)_k = 1 + \log \eta_k,$$

$$\begin{aligned}\ell(\eta, i) &= \langle 1 + \log \eta, \eta \rangle - 1 - \log \eta_i - \sum_{k=1}^K \eta_k \log \eta_k = \\ &= \sum_{k=1}^K \eta_k \log \eta_k + 1 - 1 - \log \eta_i - \sum_{k=1}^K \eta_k \log \eta_k = -\log \eta_i,\end{aligned}$$

$$\begin{aligned}\mathbf{R}_{\text{Tot}} &= \sum_{k=1}^K \left((1 + \log \hat{\eta}_k) \hat{\eta}_k - \hat{\eta}_k \log \hat{\eta}_k - (1 + \log \hat{\eta}_k) \eta_k \right) = \\ &= \sum_{k=1}^K \left(\hat{\eta}_k \log \hat{\eta}_k - \hat{\eta}_k \log \hat{\eta}_k - \eta_k \log \hat{\eta}_k \right) = \text{CE}[\eta \parallel \hat{\eta}],\end{aligned}$$

$$\mathbf{R}_{\text{Bayes}} = -\sum_{k=1}^K \eta_k \log \eta_k = \mathbb{H}\eta,$$

$$\mathbf{R}_{\text{Exc}} = \mathbf{R}_{\text{Tot}} - \mathbf{R}_{\text{Bayes}} = \text{CE}[\eta \parallel \hat{\eta}] - \mathbb{H}\eta = \text{KL}[\eta \parallel \hat{\eta}].$$

D.2 QUADRATIC SCORE (BRIER SCORE)

$$G(\eta) = -\sum_{k=1}^K \eta_k (1 - \eta_k),$$

$$G'(\eta)_k = 2\eta_k - 1,$$

$$\begin{aligned}\ell(\eta, i) &= \langle 2\eta - 1, \eta \rangle - 2\eta_i + 1 + \sum_{k=1}^K \eta_k (1 - \eta_k) = \\ &= 2 \sum_{k=1}^K \eta_k^2 - 1 - 2\eta_i + 1 + 1 - \sum_{k=1}^K \eta_k^2 = \sum_{k=1}^K \eta_k^2 - 2\eta_i + 1,\end{aligned}$$

since constant does not affect optimization, we will use the following:

$$\ell(\eta, i) = \sum_{k=1}^K \eta_k^2 - 2\eta_i.$$

$$\begin{aligned} \mathbf{R}_{\text{Tot}} &= \sum_{k=1}^K (2\hat{\eta}_k - 1)\hat{\eta}_k + \sum_{k=1}^K \hat{\eta}_k(1 - \hat{\eta}_k) - \sum_{k=1}^K (2\hat{\eta}_k - 1)\eta_k = \\ &= \sum_{k=1}^K (\hat{\eta}_k^2 - 2\hat{\eta}_k\eta_k + \eta_k^2 - \eta_k^2) + 1 = \|\hat{\eta} - \eta\|_2^2 - \|\eta\|_2^2 + 1, \\ \mathbf{R}_{\text{Bayes}} &= \sum_{k=1}^K \eta_k(1 - \eta_k) = 1 - \|\eta_k\|_2^2, \\ \mathbf{R}_{\text{Exc}} &= \mathbf{R}_{\text{Tot}} - \mathbf{R}_{\text{Bayes}} = \|\hat{\eta} - \eta\|_2^2 - \|\eta\|_2^2 + 1 - 1 + \|\eta_k\|_2^2 = \|\hat{\eta} - \eta\|_2^2. \end{aligned}$$

D.3 ZERO-ONE SCORE

$$G(\eta) = \max_k \eta_k - 1,$$

$$G'(\eta)_k = \mathbb{I}[k = \arg \max_j \eta_j],$$

$$\begin{aligned} \ell(\eta, i) &= \langle \mathbb{I}[k = \arg \max_j \eta_j], \eta \rangle - \mathbb{I}[i = \arg \max_j \eta_j] - \max_k \eta_k + 1 = \\ &= \max_k \eta_k - \mathbb{I}[i = \arg \max_j \eta_j] - \max_k \eta_k + 1 = 1 - \mathbb{I}[i = \arg \max_j \eta_j] = \mathbb{I}[i \neq \arg \max_j \eta_j], \end{aligned}$$

$$\begin{aligned} \mathbf{R}_{\text{Tot}} &= \sum_{k=1}^K \left(\hat{\eta}_k \mathbb{I}[k = \arg \max_j \hat{\eta}_k] - \eta_k \mathbb{I}[k = \arg \max_j \hat{\eta}_k] \right) - \max_k \hat{\eta}_k + 1 = \\ &= \max_k \hat{\eta}_k - \eta_{\arg \max_j \hat{\eta}_k} - \max_k \hat{\eta}_k + 1 = 1 - \eta_{\arg \max_j \hat{\eta}_k}, \\ \mathbf{R}_{\text{Bayes}} &= 1 - \max_k \eta_k, \\ \mathbf{R}_{\text{Exc}} &= \mathbf{R}_{\text{Tot}} - \mathbf{R}_{\text{Bayes}} = 1 - \eta_{\arg \max_j \hat{\eta}_k} - 1 + \max_k \eta_k = \eta_{\arg \max_j \eta_k} - \eta_{\arg \max_j \hat{\eta}_k}. \end{aligned}$$

D.4 SPHERICAL SCORE

$$G(\eta) = \|\eta\|_2 - 1,$$

$$G'(\eta)_k = \frac{\eta_k}{\|\eta\|_2},$$

$$\ell(\eta, i) = \left\langle \frac{\eta}{\|\eta\|_2}, \eta \right\rangle - \frac{\eta_i}{\|\eta\|_2} - \|\eta\|_2 + 1 = \|\eta\|_2 - \frac{\eta_i}{\|\eta\|_2} - \|\eta\|_2 + 1 = 1 - \frac{\eta_i}{\|\eta\|_2},$$

$$\mathbf{R}_{\text{Tot}} = \sum_{k=1}^K \left(\frac{\hat{\eta}_k \hat{\eta}_k}{\|\hat{\eta}\|_2} - \frac{\eta_k \hat{\eta}_k}{\|\hat{\eta}\|_2} \right) - \|\hat{\eta}\|_2 + 1 = 1 - \sum_{k=1}^K \frac{\eta_k \hat{\eta}_k}{\|\hat{\eta}\|_2} = 1 - \|\eta\|_2 \left\langle \frac{\eta}{\|\eta\|_2}, \frac{\hat{\eta}}{\|\hat{\eta}\|_2} \right\rangle,$$

$$\mathbf{R}_{\text{Bayes}} = 1 - \|\eta\|_2,$$

$$\mathbf{R}_{\text{Exc}} = \mathbf{R}_{\text{Tot}} - \mathbf{R}_{\text{Bayes}} = 1 - \|\eta\|_2 \left\langle \frac{\eta}{\|\eta\|_2}, \frac{\hat{\eta}}{\|\hat{\eta}\|_2} \right\rangle + \|\eta\|_2 - 1 = \|\eta\|_2 \left(1 - \left\langle \frac{\eta}{\|\eta\|_2}, \frac{\hat{\eta}}{\|\hat{\eta}\|_2} \right\rangle \right).$$

918 D.5 NEGATIVE LOG SCORE
919

920
$$G(\eta) = - \sum_{k=1}^K \log \eta_k,$$

921
$$G'(\eta)_k = - \frac{1}{\eta_k},$$

922
$$\ell(\eta, i) = \left\langle -\frac{1}{\eta}, \eta \right\rangle + \frac{1}{\eta_i} + \sum_{k=1}^K \log \eta_k = -K + \frac{1}{\eta_i} + \sum_{k=1}^K \log \eta_k,$$

923 since constant does not affect optimization, we will have:
924

925
$$\ell(\eta, i) = \frac{1}{\eta_k} + \sum_{k=1}^K \log \eta_k,$$

926
$$\mathbf{R}_{\text{Tot}} = \sum_{k=1}^K \left(-\frac{\hat{\eta}_k}{\hat{\eta}_k} + \frac{\eta_k}{\hat{\eta}_k} + \log \hat{\eta}_k \right) = \sum_{k=1}^K \left(\frac{\eta_k}{\hat{\eta}_k} + \log \hat{\eta}_k - 1 \right),$$

927
$$\mathbf{R}_{\text{Bayes}} = \sum_{k=1}^K \log \eta_k,$$

928
$$\mathbf{R}_{\text{Exc}} = \mathbf{R}_{\text{Tot}} - \mathbf{R}_{\text{Bayes}} = \sum_{k=1}^K \left(\frac{\eta_k}{\hat{\eta}_k} + \log \hat{\eta}_k - 1 - \log \eta_k \right) = \sum_{k=1}^K \left(\frac{\eta_k}{\hat{\eta}_k} - \log \frac{\eta_k}{\hat{\eta}_k} - 1 \right) = D_{\text{IS}}[\eta \| \hat{\eta}].$$

929
930
931
932
933
934
935
936
937
938
939
940
941
942
943 E IS THERE THE BEST APPROXIMATION?
944

945 We discussed the choice of the approximation for Bayes risk in the main part of the paper. Here, we
946 discuss whether there is a best choice of Excess risk. If we know it, we can choose the best Total risk.
947

948 Recall that for Excess risk there are 9 possible options:
949

- 950 • **Expected Pairwise Bregman Divergence (EPBD):**

951
$$\tilde{\mathbf{R}}_{\text{Exc}}^{(1,1)}(x) = \mathbb{E}_{p(\bar{\theta}|D_{tr})} \mathbb{E}_{p(\theta|D_{tr})} D_G(\eta_{\bar{\theta}} \| \eta_{\theta}).$$

952 Note, that since KL divergence is a special case of Bregman divergence, Expected Pairwise
953 KL (EPKL (Malinin & Gales, 2021; Schweighofer et al., 2023a)) is one of the special cases
954 of this Excess risk estimate.
955

- 956 • **Bregman Information (BI):**

957
$$\tilde{\mathbf{R}}_{\text{Exc}}^{(1,2)}(x) = \mathbb{E}_{p(\bar{\theta}|D_{tr})} D_G(\eta_{\bar{\theta}} \| \hat{\eta}_{D_{tr}}),$$

958 which special case is BALD (Gal et al., 2017; Houlby et al., 2011).
959

- 960 • **Reverse Bregman Information (RBI):**

961
$$\tilde{\mathbf{R}}_{\text{Exc}}^{(2,1)}(x) = \mathbb{E}_{p(\theta|D_{tr})} D_G(\hat{\eta}_{D_{tr}} \| \eta_{\theta}).$$

962 Its special case for Log score is known as **Reverse Mutual Information** (Malinin & Gales,
963 2021).
964

- 965 • **Modified Bregman Information (MBI):**

966
$$\tilde{\mathbf{R}}_{\text{Exc}}^{(1,3)}(x) = \mathbb{E}_{p(\theta|D_{tr})} D_G(\eta_{\theta} \| \bar{\eta}).$$

967 It is similar to Bregman Information, but the deviation is computed from the “central
968 prediction”, not central label (BMA).
969
970
971

972
973
974
975
976
977
978
979
980
981
982
983
984
985
986
987
988
989
990
991
992
993
994
995
996
997
998
999
1000
1001
1002
1003
1004
1005
1006
1007
1008
1009
1010
1011
1012
1013
1014
1015
1016
1017
1018
1019
1020
1021
1022
1023
1024
1025

- **Modified Reverse Bregman Information (MRBI):**

$$\tilde{R}_{\text{Exc}}^{(3,1)}(x) = \mathbb{E}_{p(\theta|D_{tr})} D_G(\hat{\eta} \parallel \eta_\theta).$$

This has similar structure to Reverse Bregman Information (RBI). Again, the deviation here is computed from another “central” prediction.

- **Forward Bias term:**

$$\tilde{R}_{\text{Exc}}^{(2,3)}(x) = D_G(\hat{\eta}_{D_{tr}} \parallel \bar{\eta}).$$

It represents a Bregman divergence between two different Bayesian estimates and can be viewed as a bias.

- **Reverse Bias term:**

$$\tilde{R}_{\text{Exc}}^{(3,2)}(x) = D_G(\bar{\eta} \parallel \hat{\eta}_{D_{tr}}).$$

This applies similar reasoning to the Forward Bias Term.

- Finally, we obtain two similar constant measures:

$$\tilde{R}_{\text{Exc}}^{(3,3)}(x) = D_G(\bar{\eta} \parallel \bar{\eta}) = 0.$$

and

$$\tilde{R}_{\text{Exc}}^{(2,2)}(x) = D_G(\hat{\eta}_{D_{tr}} \parallel \hat{\eta}_{D_{tr}}) = 0,$$

which is coherent with the result obtained for the Total risk, when Excess risk (epistemic uncertainty) is equal to 0.

However, it is not clear, what estimate of the Excess risk we should use. Indeed, neither of these estimates are upper nor lower bounds for the true Excess risk. This is because contrary to Bayes risk, we don't have any idea if Excess risk with ground truth η reaches any extreme. For another explanation, see Figure 2 and discussion in Section B. For simplicity, we will consider only approximations with strategies (1) and (2), as for them we know, at least, which estimate of Bayes risk is better.

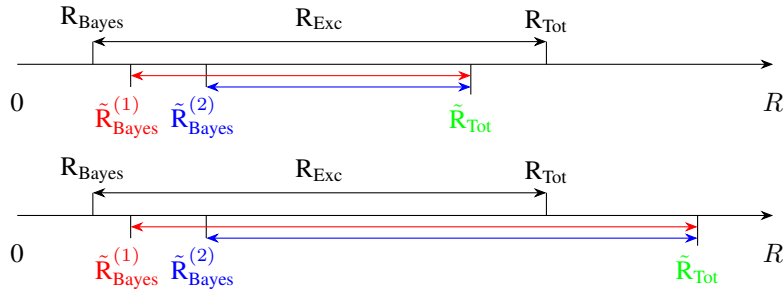


Figure 2: Different situations for risk estimates. Risks typed in black and above the axis are the true ones. Risks, typed in color, and below are estimates. Two-pointed arrows show Excess risks.

Top. \tilde{R}_{Tot} underestimates R_{Tot} , $\tilde{R}_{\text{Bayes}}^{(1)}$ better estimates R_{Bayes} , and $\tilde{R}_{\text{Exc}}^{(1)}$ better estimates R_{Exc} .

Bottom. \tilde{R}_{Tot} overestimates R_{Tot} , $\tilde{R}_{\text{Bayes}}^{(1)}$ better estimates R_{Bayes} , and $\tilde{R}_{\text{Exc}}^{(2)}$ better estimates R_{Exc} . We see, that for different estimates of R_{Tot} , we have different best approximations for R_{Exc} . See discussion in Section B.

In Figure 2, for simplicity, we consider only the Bayesian approximation of the first argument (ground-truth probability). In black, we have actual (real risks), while in color we have different estimates of risks. Also, as two-sided arrows, we show the Excess risk.

If we *underestimate* the Total risk (see top plot in Figure 2), the best choice for Excess risk will be $\tilde{R}_{\text{Exc}}^{(1)}$, as despite being a lower bound on Excess risk, it is the best we can do ($\tilde{R}_{\text{Exc}}^{(2)}$ in this case will be even worse). However, if we *overestimate* Total risk, then there is no single best choice. In the bottom plot, when \tilde{R}_{Tot} significantly overestimates R_{Tot} , the second idea for estimating Excess risk gives a better estimate, despite the first idea for Bayes risk still better.

Hence, the best estimate of Excess risk depends on how well we estimate Total risk. But we never know in advance for a particular input x , in which regime (overestimated or underestimated Total risk) we are. Thus, there is no best choice among these risks to approximate epistemic uncertainty.

F RELATIONS BETWEEN THE ESTIMATES

In this section, we discuss how the measures of uncertainty are connected. In the main text, we discussed several ways how one can estimate risk given an ensemble of models, posterior, or samples from it. In what follows, we show how one can further decompose these estimates of Excess risk.

Let us start with $\tilde{\mathbf{R}}_{\text{Exc}}^{(1,1)}(x)$. Using results of (Pfau, 2013), we have:

$$\begin{aligned}\tilde{\mathbf{R}}_{\text{Exc}}^{(1,1)}(x) &= \mathbb{E}_{p(\theta|D_{tr})} \mathbb{E}_{p(\tilde{\theta}|D_{tr})} D_G(\eta_{\tilde{\theta}} \| \eta_{\theta}) = \\ &\mathbb{E}_{p(\theta|D_{tr})} D_G(\hat{\eta}_{D_{tr}} \| \eta_{\theta}) + \mathbb{E}_{p(\tilde{\theta}|D_{tr})} D_G(\eta_{\tilde{\theta}} \| \hat{\eta}_{D_{tr}}) = \tilde{\mathbf{R}}_{\text{Exc}}^{(2,1)}(x) + \tilde{\mathbf{R}}_{\text{Exc}}^{(1,2)}(x).\end{aligned}$$

Since all of these estimates are non-negative, the following holds true:

$$\tilde{\mathbf{R}}_{\text{Exc}}^{(1,1)}(x) \geq \tilde{\mathbf{R}}_{\text{Exc}}^{(2,1)}(x) \geq \tilde{\mathbf{R}}_{\text{Exc}}^{(2,2)}(x) = 0,$$

and

$$\tilde{\mathbf{R}}_{\text{Exc}}^{(1,1)}(x) \geq \tilde{\mathbf{R}}_{\text{Exc}}^{(1,2)}(x) \geq \tilde{\mathbf{R}}_{\text{Exc}}^{(2,2)}(x) = 0$$

for any x .

Moreover, one can show that the following holds:

$$\begin{aligned}\tilde{\mathbf{R}}_{\text{Tot}}^{(1,1)}(x) &= \tilde{\mathbf{R}}_{\text{Tot}}^{(2,1)}(x) = \tilde{\mathbf{R}}_{\text{Bayes}}^{(1)}(x) + \tilde{\mathbf{R}}_{\text{Exc}}^{(1,1)}(x) = \tilde{\mathbf{R}}_{\text{Bayes}}^{(2)}(x) + \tilde{\mathbf{R}}_{\text{Exc}}^{(2,1)}(x), \\ \tilde{\mathbf{R}}_{\text{Tot}}^{(1,2)}(x) &= \tilde{\mathbf{R}}_{\text{Tot}}^{(2,2)}(x) = \tilde{\mathbf{R}}_{\text{Bayes}}^{(2)}(x) + \tilde{\mathbf{R}}_{\text{Exc}}^{(2,2)}(x) = \tilde{\mathbf{R}}_{\text{Bayes}}^{(1)}(x) + \tilde{\mathbf{R}}_{\text{Exc}}^{(1,2)}(x). \\ \tilde{\mathbf{R}}_{\text{Tot}}^{(3,3)}(x) &= \tilde{\mathbf{R}}_{\text{Bayes}}^{(3)}(x) + \tilde{\mathbf{R}}_{\text{Exc}}^{(3,3)}(x) = \tilde{\mathbf{R}}_{\text{Bayes}}^{(3)}(x) = \tilde{\mathbf{R}}_{\text{Tot}}^{(3,1)}(x) - \tilde{\mathbf{R}}_{\text{Exc}}^{(3,1)}(x).\end{aligned}$$

$$\tilde{\mathbf{R}}_{\text{Tot}}^{(1,3)}(x) = \tilde{\mathbf{R}}_{\text{Tot}}^{(2,3)}(x) = \tilde{\mathbf{R}}_{\text{Tot}}^{(2,1)}(x) - \tilde{\mathbf{R}}_{\text{Exc}}^{(3,1)}(x).$$

From Pfau (2013) the following holds:

$$\tilde{\mathbf{R}}_{\text{Exc}}^{(2,1)}(x) = \tilde{\mathbf{R}}_{\text{Exc}}^{(2,3)}(x) + \tilde{\mathbf{R}}_{\text{Exc}}^{(3,1)}(x). \quad (9)$$

Additionally, Bregman information can be received as follows:

$$BI(x) = \tilde{\mathbf{R}}_{\text{Exc}}^{(1,1)}(x) - \tilde{\mathbf{R}}_{\text{Exc}}^{(2,1)}(x) = \tilde{\mathbf{R}}_{\text{Exc}}^{(1,2)}(x) - \tilde{\mathbf{R}}_{\text{Exc}}^{(2,2)}(x) = \tilde{\mathbf{R}}_{\text{Bayes}}^{(2)}(x) - \tilde{\mathbf{R}}_{\text{Bayes}}^{(1)}(x). \quad (10)$$

Reverse Bregman Information:

$$RBI(x) = \tilde{\mathbf{R}}_{\text{Exc}}^{(2,1)}(x) - \tilde{\mathbf{R}}_{\text{Exc}}^{(2,2)}(x) = \tilde{\mathbf{R}}_{\text{Exc}}^{(1,1)}(x) - \tilde{\mathbf{R}}_{\text{Exc}}^{(1,2)}(x) = \tilde{\mathbf{R}}_{\text{Tot}}^{(1,1)}(x) - \tilde{\mathbf{R}}_{\text{Tot}}^{(1,2)}(x).$$

Interestingly, the EPBD can be written in two equivalent forms:

$$\tilde{\mathbf{R}}_{\text{Exc}}^{(1,1)}(x) = \tilde{\mathbf{R}}_{\text{Exc}}^{(1,2)}(x) + \tilde{\mathbf{R}}_{\text{Exc}}^{(2,1)}(x) = \tilde{\mathbf{R}}_{\text{Exc}}^{(1,3)}(x) + \tilde{\mathbf{R}}_{\text{Exc}}^{(3,1)}(x). \quad (11)$$

An interesting observation from the (11) is that in general there are two central points: central label and central prediction—where the sum of expected deviations in terms of Bregman divergence lead to the same result, known as EPBD. To the best of our knowledge, this is a novel finding.

Now we are fully equipped to recover the decomposition, used in Gruber & Buettner (2023) (Equation (8)), which is naturally appears, when using $\tilde{\mathbf{R}}_{\text{Tot}}^{(1,1)}$ from the above, as well as Equation (9) and Equation (10).

G CONNECTION TO ENERGY-BASED MODELS

Here, we will consider a specific case of the framework, instantiated for Logscore. In what follows, we will sometimes omit explicit dependency on x for better presentation. However, this dependency is always assumed.

Recap, that for the special case of Logscore, Bregman divergence is Kullback-Leibler divergence.

Hence, $\tilde{\mathbf{R}}_{\text{Exc}}^{(3,1)} = \mathbb{E}_\theta \text{KL}(\bar{\eta} \mid \eta_\theta)$. Using results from Table 1, we can derive that:

$$\log \bar{\eta}_i = \left[\mathbb{E}_\theta \log \eta_\theta \right]_i - \log \sum_j \exp \left[\mathbb{E}_\theta \log \eta_\theta \right]_j.$$

Moreover $\frac{f_\theta(x)}{T} = \text{Softmax}^{-1}(\eta_\theta(x))$, where T is temperature, that scales logits $f_\theta(x)$.

Hence, the logarithm of a probability vector can be further expanded:

$$\left[\log \eta_\theta \right]_i = \log \frac{\left[\exp \frac{f_\theta}{T} \right]_i}{\sum_j \left[\exp \frac{f_\theta}{T} \right]_j} = \left[\frac{f_\theta}{T} \right]_i - \log \sum_j \exp \left[\frac{f_\theta}{T} \right]_j.$$

From these equations, we can derive:

$$\begin{aligned} \tilde{\mathbf{R}}_{\text{Exc}}^{(3,1)} &= \mathbb{E}_\theta \text{KL}(\bar{\eta} \mid \eta_\theta) = \mathbb{E}_\theta \sum_i \bar{\eta}_i \left[\log \frac{\bar{\eta}}{\eta_\theta} \right]_i = \sum_i \bar{\eta}_i \log \bar{\eta}_i - \sum_i \bar{\eta}_i \left[\mathbb{E}_\theta \log \eta_\theta \right]_i = \\ &= \sum_i \bar{\eta}_i \left[\mathbb{E}_\theta \log \eta_\theta \right]_i - \sum_i \bar{\eta}_i \log \sum_j \exp \left[\mathbb{E}_\theta \log \eta_\theta \right]_j - \sum_i \bar{\eta}_i \left[\mathbb{E}_\theta \log \eta_\theta \right]_i = \\ &= - \log \sum_j \exp \left[\mathbb{E}_\theta \log \eta_\theta \right]_j, \end{aligned}$$

Furthermore, one may show that:

$$\begin{aligned} \tilde{\mathbf{R}}_{\text{Exc}}^{(3,1)} &= - \log \sum_i \exp \left[\mathbb{E}_\theta \log \eta_\theta \right]_i = - \log \sum_i \exp \left[\left[\frac{\mathbb{E}_\theta f_\theta}{T} \right]_i - \mathbb{E}_\theta \log \sum_j \exp \left[\frac{f_\theta}{T} \right]_j \right] = \\ &= - \log \frac{\sum_i \exp \left[\frac{\mathbb{E}_\theta f_\theta}{T} \right]_i}{\exp \mathbb{E}_\theta \log \sum_j \exp \left[\frac{f_\theta}{T} \right]_j} = - \log \sum_i \exp \left[\frac{\mathbb{E}_\theta f_\theta}{T} \right]_i + \mathbb{E}_\theta \log \sum_j \exp \left[\frac{f_\theta}{T} \right]_j = \\ &= \frac{1}{T} \left(-T \log \sum_i \exp \left[\frac{\mathbb{E}_\theta f_\theta}{T} \right]_i - \left[-T \mathbb{E}_\theta \log \sum_j \exp \left[\frac{f_\theta}{T} \right]_j \right] \right). \end{aligned}$$

Hence:

$$T \tilde{\mathbf{R}}_{\text{Exc}}^{(3,1)}(x) = \underbrace{-T \log \sum_i \exp \left[\frac{\mathbb{E}_\theta f_\theta}{T} \right]_i}_{E(x; \mathbb{E}_\theta f_\theta)} - \underbrace{\left(-T \mathbb{E}_\theta \log \sum_j \exp \left[\frac{f_\theta}{T} \right]_j \right)}_{\mathbb{E}_\theta E(x; f_\theta)}.$$

Therefore,

$$\tilde{\mathbf{R}}_{\text{Exc}}^{(3,1)}(x) = \frac{1}{T} \left(E(x; \mathbb{E}_\theta f_\theta) - \mathbb{E}_\theta E(x; f_\theta) \right).$$

Next, we can consider another approximation, namely $\tilde{\mathbf{R}}_{\text{Exc}}^{(1,3)}$:

$$\begin{aligned}
\tilde{\mathbf{R}}_{\text{Exc}}^{(1,3)} &= \mathbb{E}_\theta \text{KL}(\eta_\theta | \bar{\eta}) = \sum_i \mathbb{E}_\theta \left[\eta_\theta \log \eta_\theta \right]_i - \sum_i \left[\mathbb{E}_\theta \eta_\theta \log \bar{\eta} \right]_i = \\
&\sum_i \mathbb{E}_\theta \left[\eta_\theta \frac{f_\theta}{T} \right]_i - \mathbb{E}_\theta \log \sum_j \exp \left[\frac{f_\theta}{T} \right]_j - \sum_i \left[\mathbb{E}_\theta \eta_\theta \mathbb{E}_\theta \log \eta_\theta \right]_i + \log \sum_j \exp \left[\mathbb{E}_\theta \log \eta_\theta \right]_j = \\
&\sum_i \mathbb{E}_\theta \left[\eta_\theta \frac{f_\theta}{T} \right]_i - \mathbb{E}_\theta \log \sum_j \exp \left[\frac{f_\theta}{T} \right]_j - \\
&\quad - \sum_i \left[\mathbb{E}_\theta \eta_\theta \mathbb{E}_\theta \left[\left[\frac{f_\theta}{T} \right]_i - \log \sum_j \exp \left[\frac{f_\theta}{T} \right]_j \right] \right] + \log \sum_j \exp \left[\mathbb{E}_\theta \log \eta_\theta \right]_j = \\
&\sum_i \mathbb{E}_\theta \left[\eta_\theta \frac{f_\theta}{T} \right]_i - \mathbb{E}_\theta \log \sum_j \exp \left[\frac{f_\theta}{T} \right]_j - \sum_i \mathbb{E}_\theta \eta_\theta \mathbb{E}_\theta \left[\frac{f_\theta}{T} \right]_i + \mathbb{E}_\theta \log \sum_j \exp \left[\frac{f_\theta}{T} \right]_j + \\
&\quad + \log \sum_j \exp \left[\mathbb{E}_\theta \log \eta_\theta \right]_j = \sum_i \text{cov} \left[[\eta_\theta]_i, \left[\frac{f_\theta}{T} \right]_i \right] + \log \sum_j \exp \left[\mathbb{E}_\theta \log \eta_\theta \right]_j = \\
&\quad \sum_i \text{cov} \left[[\eta_\theta]_i, \left[\frac{f_\theta}{T} \right]_i \right] - \tilde{\mathbf{R}}_{\text{Exc}}^{(3,1)}.
\end{aligned}$$

Therefore,

$$\tilde{\mathbf{R}}_{\text{Exc}}^{(1,3)} + \tilde{\mathbf{R}}_{\text{Exc}}^{(3,1)} = \tilde{\mathbf{R}}_{\text{Exc}}^{(1,1)} = \sum_i \text{cov} \left[[\eta_\theta]_i, \left[\frac{f_\theta}{T} \right]_i \right].$$

Therefore, Expected Pairwise Kullback-Leibler divergence (EPBD in the partial case of Logscore) is equal to the sum of covariances, between predicted probability of a class, and the corresponding scaled (tempered) logit. To our best knowledge, it is the first interpretation of the result.

H TRAINING DETAILS

Training procedures for each dataset were similar. We used ResNet18 architecture. **All the networks in the ensemble were trained entirely independently, each starting from a different random initialization of weights. They did not share any parameters.**

For CIFAR10-based datasets, we used code from this repository: <https://github.com/kuangliu/pytorch-cifar>. The training procedure consisted of 200 epochs with a cosine annealing learning rate. For an optimizer, we use SGD with momentum and weight decay. For more details see the code.

In Figure 3 (left) we present performance summary statistics of the ensembles. Specifically, we show accuracy, macro averaged precision, recall, and F1-score.

For CIFAR100-based datasets, we used code from this repository: <https://github.com/weiaicunzai/pytorch-cifar100>. The training procedure consisted of 200 epochs with learning rate decay at particular milestones: [60, 120, 160]. For an optimizer, we use SGD with momentum and weight decay. For more details see the code.

Similarly to CIFAR10, in Figure 3 (middle) we present performance summary statistics of the ensembles of ResNet18 architecture.

For TinyImageNet, we used pre-trained models, provided by Torch-Uncertainty team <https://github.com/ENSTA-U2IS-AI/torch-uncertainty>. They are provided with a single training loss function. Training statistics for this dataset are in Figure 3 (right).

Please note, that for all these datasets, we used different loss functions during training and various instantiations of G for the uncertainty quantification measures. The specific configurations are specified in the captions of the result tables.

1188
 1189
 1190
 1191
 1192
 1193
 1194
 1195
 1196
 1197
 1198
 1199
 1200
 1201
 1202
 1203
 1204
 1205
 1206
 1207
 1208
 1209
 1210
 1211
 1212
 1213
 1214
 1215
 1216
 1217
 1218
 1219
 1220
 1221
 1222
 1223
 1224
 1225
 1226
 1227
 1228
 1229
 1230
 1231
 1232
 1233
 1234
 1235
 1236
 1237
 1238
 1239
 1240
 1241

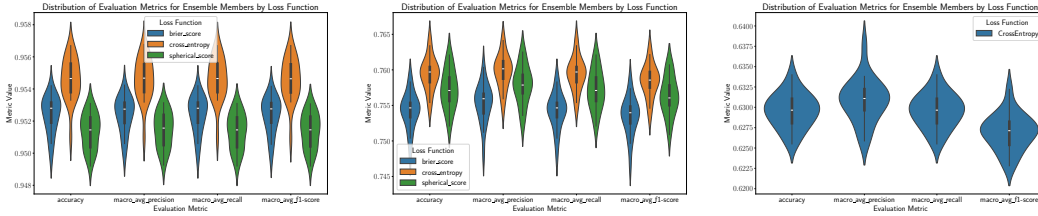


Figure 3: Violin plots for different training loss functions and different metrics for ResNet18 Left: CIFAR10; Middle: CIFAR100; Right: TinyImageNet.

I DESCRIPTION OF DATASETS

I.1 NOISY DATASETS

In this section, we describe the noisy versions of CIFAR10 and CIFAR100 datasets created for our experiments, namely CIFAR10-N and CIFAR100-N (N stands for “noisy”).

In the datasets, the images are the same as in the original dataset (covariates are not changed). However, some of the labels are randomly swapped. Hence, only labels were changed, while covariates were kept as in the original dataset. The motivation for the creation of this dataset is due to the fact that conventional image classification datasets essentially contain no aleatoric uncertainty (Kapoor et al., 2022). To mitigate the limitation, which is critical for our evaluation, we introduce the label noise manually. By nature, this noise is aleatoric.

CIFAR10-N. We decide to do the following pairs of labels that are randomly swapped: 1 to 7, 7 to 1, 3 to 8, 8 to 3, 2 to 5, and 5 to 2.

CIFAR100-N. We decided to randomly swap the following pairs of labels: 1 to 7, 7 to 1, 3 to 8, 8 to 3, 2 to 5, 5 to 2, 10 to 20, 20 to 10, 40 to 50, 50 to 40, 90 to 99, 99 to 90, 25 to 75, 75 to 25, 17 to 71, 71 to 17, 13 to 31, 31 to 13, and 24 to 42, 42 to 24.

Both these noisy datasets were used in training. When evaluating misclassification detection, we use original versions of these datasets.

I.2 IMAGENET DATASETS

Here we present descriptions of variations of ImageNet datasets we have used.

ImageNet-A ImageNet-A (Hendrycks et al., 2021b) is dataset very similar to ImageNet test set, but proven to be more challenging for existing classification models. It contains real-world, unmodified, and naturally occurring examples that are misclassified by ResNet models.

ImageNet-O Closely related to ImageNet-A, ImageNet-O (Hendrycks et al., 2021b) is dataset that contains real-world examples, with classes that are not present in standard ImageNet dataset. It can be used to test out of distribution detection.

ImageNet-R This dataset contains renditions of 200 classes from ImageNet (Hendrycks et al., 2021a). Artistic rendition introduces a significant distribution shift and present a challenging task for classification models. It can be used to test robustness of model and out of distribution detection.

J ADDITIONAL EXPERIMENTS ON OUT-OF-DISTRIBUTION DETECTION

In this section, we provide additional experiments on out-of-distribution detection. Here, we use different instantiations of G for loss function and for uncertainty quantification, as well as try different in-distribution datasets. Results for CIFAR10 are in Tables 5, 6 and 7. For CIFAR100, additional

Table 5: AUROC for out-of-distribution detection for CIFAR10 (in-distribution). As a loss function for training and for uncertainty quantification we used **Log Score**.

	CIFAR100	SVHN	TinyImageNet	CIFAR10C-1	CIFAR10C-2	CIFAR10C-3	CIFAR10C-4	CIFAR10C-5
LogScore $\bar{R}_{\text{Bayes}}^{(3)}$	90.93 ± 0.03	95.76 ± 0.41	90.35 ± 0.07	60.66 ± 0.11	67.44 ± 0.11	72.14 ± 0.09	76.82 ± 0.09	82.93 ± 0.14
LogScore $\bar{R}_{\text{Bayes}}^{(2)}$	91.3 ± 0.05	96.06 ± 0.49	90.67 ± 0.04	60.98 ± 0.1	67.87 ± 0.09	72.61 ± 0.08	77.33 ± 0.09	83.48 ± 0.15
LogScore $\bar{R}_{\text{Bayes}}^{(1)}$	91.36 ± 0.05	96.01 ± 0.39	90.84 ± 0.04	60.96 ± 0.09	67.84 ± 0.09	72.59 ± 0.08	77.31 ± 0.08	83.48 ± 0.13
LogScore $\bar{R}_{\text{Exc}}^{(3,3)}$	50.0 ± 0.0	50.0 ± 0.0	50.0 ± 0.0	50.0 ± 0.0	50.0 ± 0.0	50.0 ± 0.0	50.0 ± 0.0	50.0 ± 0.0
LogScore $\bar{R}_{\text{Exc}}^{(3,2)}$	89.08 ± 0.14	92.57 ± 1.18	88.15 ± 0.13	60.87 ± 0.12	67.46 ± 0.1	72.04 ± 0.09	76.58 ± 0.12	82.24 ± 0.18
LogScore $\bar{R}_{\text{Exc}}^{(3,1)}$	90.38 ± 0.06	94.31 ± 0.91	89.54 ± 0.06	61.09 ± 0.11	67.86 ± 0.09	72.54 ± 0.09	77.22 ± 0.13	83.11 ± 0.19
LogScore $\bar{R}_{\text{Exc}}^{(2,3)}$	88.64 ± 0.15	91.95 ± 1.18	87.68 ± 0.13	60.82 ± 0.12	67.36 ± 0.09	71.89 ± 0.08	76.38 ± 0.12	81.94 ± 0.18
LogScore $\bar{R}_{\text{Exc}}^{(2,2)}$	50.0 ± 0.0	50.0 ± 0.0	50.0 ± 0.0	50.0 ± 0.0	50.0 ± 0.0	50.0 ± 0.0	50.0 ± 0.0	50.0 ± 0.0
LogScore $\bar{R}_{\text{Exc}}^{(2,1)}$	90.06 ± 0.06	93.92 ± 1.06	89.19 ± 0.07	61.06 ± 0.11	67.8 ± 0.09	72.45 ± 0.08	77.1 ± 0.13	82.93 ± 0.2
LogScore $\bar{R}_{\text{Exc}}^{(1,3)}$	89.99 ± 0.08	93.84 ± 1.06	89.12 ± 0.07	61.06 ± 0.11	67.79 ± 0.09	72.43 ± 0.08	77.07 ± 0.13	82.9 ± 0.2
LogScore $\bar{R}_{\text{Exc}}^{(1,2)}$	90.38 ± 0.08	94.35 ± 0.94	89.57 ± 0.07	61.1 ± 0.11	67.87 ± 0.09	72.55 ± 0.09	77.23 ± 0.13	83.14 ± 0.2
LogScore $\bar{R}_{\text{Exc}}^{(1,1)}$	90.17 ± 0.06	94.08 ± 1.02	89.32 ± 0.07	61.07 ± 0.11	67.82 ± 0.09	72.49 ± 0.08	77.15 ± 0.13	83.0 ± 0.2
LogScore $\bar{R}_{\text{Tot}}^{(3,3)}$	90.93 ± 0.03	95.76 ± 0.41	90.35 ± 0.07	60.66 ± 0.11	67.44 ± 0.11	72.14 ± 0.09	76.82 ± 0.09	82.93 ± 0.14
LogScore $\bar{R}_{\text{Tot}}^{(3,2)}$	90.95 ± 0.04	95.8 ± 0.44	90.33 ± 0.06	60.7 ± 0.11	67.49 ± 0.1	72.19 ± 0.09	76.88 ± 0.09	83.0 ± 0.15
LogScore $\bar{R}_{\text{Tot}}^{(3,1)}$	90.72 ± 0.04	95.44 ± 0.53	90.03 ± 0.06	60.71 ± 0.11	67.49 ± 0.1	72.17 ± 0.09	76.83 ± 0.1	82.88 ± 0.17
LogScore $\bar{R}_{\text{Tot}}^{(2,3)}$	91.15 ± 0.05	95.91 ± 0.56	90.49 ± 0.04	60.98 ± 0.09	67.85 ± 0.09	72.58 ± 0.08	77.29 ± 0.09	83.41 ± 0.17
LogScore $\bar{R}_{\text{Tot}}^{(2,2)}$	91.3 ± 0.05	96.06 ± 0.49	90.67 ± 0.04	60.98 ± 0.1	67.87 ± 0.09	72.61 ± 0.08	77.33 ± 0.09	83.48 ± 0.15
LogScore $\bar{R}_{\text{Tot}}^{(2,1)}$	90.81 ± 0.04	95.39 ± 0.71	90.06 ± 0.05	60.96 ± 0.1	67.8 ± 0.1	72.49 ± 0.09	77.16 ± 0.11	83.18 ± 0.19
LogScore $\bar{R}_{\text{Tot}}^{(1,3)}$	91.15 ± 0.05	95.91 ± 0.56	90.49 ± 0.04	60.98 ± 0.09	67.85 ± 0.09	72.58 ± 0.08	77.29 ± 0.09	83.41 ± 0.17
LogScore $\bar{R}_{\text{Tot}}^{(1,2)}$	91.3 ± 0.05	96.06 ± 0.49	90.67 ± 0.04	60.98 ± 0.1	67.87 ± 0.09	72.61 ± 0.08	77.33 ± 0.09	83.48 ± 0.15
LogScore $\bar{R}_{\text{Tot}}^{(1,1)}$	90.81 ± 0.04	95.39 ± 0.71	90.06 ± 0.05	60.96 ± 0.1	67.8 ± 0.1	72.49 ± 0.09	77.16 ± 0.11	83.18 ± 0.19
LogScore $E(x; \mathbb{E}_\theta f_\theta)$	91.12 ± 0.02	96.69 ± 0.34	90.68 ± 0.05	60.61 ± 0.13	67.46 ± 0.14	72.25 ± 0.12	76.97 ± 0.12	83.22 ± 0.18
LogScore $\mathbb{E}_\theta E(x; f_\theta)$	91.1 ± 0.01	96.56 ± 0.44	90.77 ± 0.04	60.6 ± 0.13	67.46 ± 0.13	72.25 ± 0.11	76.96 ± 0.11	83.21 ± 0.16

results are in Table 8. For TinyImageNet, results are in Table 9. In all these experiments, we computed energy scores only for Log score, as these terms naturally appear only for this instantiation.

Note, that for CIFAR10 and CIFAR100, we used matching function G for the loss function and for uncertainty quantification. For TinyImageNet, we had only one loss function, and we apply different instantiations of G only for the evaluation of uncertainty measures.

From all these tables one can observe, that Log Score-based measures typically outperform others, that justifies them as a popular practical choice in uncertainty quantification problems. Also, we see that for “hard-OOD” datasets, Bayes (and Total) risks usually perform better, than Excess risk. In “soft-OOD” cases, such as CIFAR10C for CIFAR10 and ImageNet-O for TinyImageNet, their performance is close, and Excess risk is a good choice.

From the results for TinyImageNet 9, we see, that matching combination of Log Score is usually better, than other instantiations. Note, that since central prediction for Zero One Score is not well defined, we excluded it from the table.

1296
1297
1298
1299
1300
1301
1302
1303
1304
1305
1306
1307
1308
1309
1310
1311
1312
1313
1314
1315
1316
1317
1318
1319
1320
1321
1322
1323
1324
1325
1326
1327
1328
1329
1330
1331
1332
1333
1334
1335
1336
1337
1338
1339
1340
1341
1342
1343
1344
1345
1346
1347
1348
1349

Table 6: AUROC for out-of-distribution detection for CIFAR10 (in-distribution). As a loss function for training and for uncertainty quantification we used **Brier Score**. Note, that due to the symmetrical nature of Brier score, many instances results to the same values.

	CIFAR100	SVHN	TinyImageNet	CIFAR10C-1	CIFAR10C-2	CIFAR10C-3	CIFAR10C-4	CIFAR10C-5
BrierScore $\bar{R}_{\text{Bayes}}^{(3)}$	90.38 ± 0.18	96.26 ± 0.34	89.71 ± 0.12	61.02 ± 0.13	68.04 ± 0.17	72.46 ± 0.19	76.82 ± 0.19	82.45 ± 0.11
BrierScore $\bar{R}_{\text{Bayes}}^{(2)}$	90.38 ± 0.18	96.26 ± 0.34	89.71 ± 0.12	61.02 ± 0.13	68.04 ± 0.17	72.46 ± 0.19	76.82 ± 0.19	82.45 ± 0.11
BrierScore $\bar{R}_{\text{Bayes}}^{(1)}$	90.44 ± 0.17	96.09 ± 0.52	89.89 ± 0.13	61.03 ± 0.12	68.04 ± 0.16	72.46 ± 0.18	76.83 ± 0.18	82.47 ± 0.1
BrierScore $\bar{R}_{\text{Exc}}^{(3,3)}$	50.0 ± 0.0	50.0 ± 0.0	50.0 ± 0.0	50.0 ± 0.0	50.0 ± 0.0	50.0 ± 0.0	50.0 ± 0.0	50.0 ± 0.0
BrierScore $\bar{R}_{\text{Exc}}^{(3,2)}$	50.0 ± 0.0	50.0 ± 0.0	50.0 ± 0.0	50.0 ± 0.0	50.0 ± 0.0	50.0 ± 0.0	50.0 ± 0.0	50.0 ± 0.0
BrierScore $\bar{R}_{\text{Exc}}^{(3,1)}$	89.24 ± 0.19	94.19 ± 0.49	88.37 ± 0.12	60.11 ± 0.15	66.59 ± 0.24	71.19 ± 0.3	75.7 ± 0.22	81.52 ± 0.16
BrierScore $\bar{R}_{\text{Exc}}^{(2,3)}$	50.0 ± 0.0	50.0 ± 0.0	50.0 ± 0.0	50.0 ± 0.0	50.0 ± 0.0	50.0 ± 0.0	50.0 ± 0.0	50.0 ± 0.0
BrierScore $\bar{R}_{\text{Exc}}^{(2,2)}$	50.0 ± 0.0	50.0 ± 0.0	50.0 ± 0.0	50.0 ± 0.0	50.0 ± 0.0	50.0 ± 0.0	50.0 ± 0.0	50.0 ± 0.0
BrierScore $\bar{R}_{\text{Exc}}^{(2,1)}$	89.24 ± 0.19	94.19 ± 0.49	88.37 ± 0.12	60.11 ± 0.15	66.59 ± 0.24	71.19 ± 0.3	75.7 ± 0.22	81.52 ± 0.16
BrierScore $\bar{R}_{\text{Exc}}^{(1,3)}$	89.24 ± 0.19	94.19 ± 0.49	88.37 ± 0.12	60.11 ± 0.15	66.59 ± 0.24	71.19 ± 0.3	75.7 ± 0.22	81.52 ± 0.16
BrierScore $\bar{R}_{\text{Exc}}^{(1,2)}$	89.24 ± 0.19	94.19 ± 0.49	88.37 ± 0.12	60.11 ± 0.15	66.59 ± 0.24	71.19 ± 0.3	75.7 ± 0.22	81.52 ± 0.16
BrierScore $\bar{R}_{\text{Exc}}^{(1,1)}$	89.24 ± 0.19	94.19 ± 0.49	88.37 ± 0.12	60.11 ± 0.15	66.59 ± 0.24	71.19 ± 0.3	75.7 ± 0.22	81.52 ± 0.16
BrierScore $\bar{R}_{\text{Tot}}^{(3,3)}$	90.38 ± 0.18	96.26 ± 0.34	89.71 ± 0.12	61.02 ± 0.13	68.04 ± 0.17	72.46 ± 0.19	76.82 ± 0.19	82.45 ± 0.11
BrierScore $\bar{R}_{\text{Tot}}^{(3,2)}$	90.38 ± 0.18	96.26 ± 0.34	89.71 ± 0.12	61.02 ± 0.13	68.04 ± 0.17	72.46 ± 0.19	76.82 ± 0.19	82.45 ± 0.11
BrierScore $\bar{R}_{\text{Tot}}^{(3,1)}$	90.04 ± 0.18	95.83 ± 0.34	89.29 ± 0.12	60.99 ± 0.13	67.98 ± 0.17	72.37 ± 0.19	76.7 ± 0.2	82.25 ± 0.13
BrierScore $\bar{R}_{\text{Tot}}^{(2,3)}$	90.38 ± 0.18	96.26 ± 0.34	89.71 ± 0.12	61.02 ± 0.13	68.04 ± 0.17	72.46 ± 0.19	76.82 ± 0.19	82.45 ± 0.11
BrierScore $\bar{R}_{\text{Tot}}^{(2,2)}$	90.38 ± 0.18	96.26 ± 0.34	89.71 ± 0.12	61.02 ± 0.13	68.04 ± 0.17	72.46 ± 0.19	76.82 ± 0.19	82.45 ± 0.11
BrierScore $\bar{R}_{\text{Tot}}^{(2,1)}$	90.04 ± 0.18	95.83 ± 0.34	89.29 ± 0.12	60.99 ± 0.13	67.98 ± 0.17	72.37 ± 0.19	76.7 ± 0.2	82.25 ± 0.13
BrierScore $\bar{R}_{\text{Tot}}^{(1,3)}$	90.38 ± 0.18	96.26 ± 0.34	89.71 ± 0.12	61.02 ± 0.13	68.04 ± 0.17	72.46 ± 0.19	76.82 ± 0.19	82.45 ± 0.11
BrierScore $\bar{R}_{\text{Tot}}^{(1,2)}$	90.38 ± 0.18	96.26 ± 0.34	89.71 ± 0.12	61.02 ± 0.13	68.04 ± 0.17	72.46 ± 0.19	76.82 ± 0.19	82.45 ± 0.11
BrierScore $\bar{R}_{\text{Tot}}^{(1,1)}$	90.04 ± 0.18	95.83 ± 0.34	89.29 ± 0.12	60.99 ± 0.13	67.98 ± 0.17	72.37 ± 0.19	76.7 ± 0.2	82.25 ± 0.13

Table 7: AUROC for out-of-distribution detection for CIFAR10 (in-distribution). As a loss function for training and for uncertainty quantification we used **Spherical Score**. Note, that due to the symmetrical nature of Brier score, many instances results to the same values.

	CIFAR100	SVHN	TinyImageNet	CIFAR10C-1	CIFAR10C-2	CIFAR10C-3	CIFAR10C-4	CIFAR10C-5
SphericalScore $\bar{R}_{\text{Bayes}}^{(3)}$	90.09 ± 0.04	95.78 ± 0.64	89.4 ± 0.18	61.42 ± 0.19	68.45 ± 0.22	72.86 ± 0.26	77.3 ± 0.31	82.89 ± 0.39
SphericalScore $\bar{R}_{\text{Bayes}}^{(2)}$	90.42 ± 0.03	96.22 ± 0.54	89.81 ± 0.18	61.46 ± 0.2	68.52 ± 0.23	72.94 ± 0.28	77.41 ± 0.33	83.03 ± 0.42
SphericalScore $\bar{R}_{\text{Bayes}}^{(1)}$	90.46 ± 0.04	96.15 ± 0.4	89.95 ± 0.19	61.47 ± 0.19	68.54 ± 0.23	72.95 ± 0.28	77.39 ± 0.34	82.99 ± 0.43
SphericalScore $\bar{R}_{\text{Exc}}^{(3,3)}$	50.0 ± 0.0	50.0 ± 0.0	50.0 ± 0.0	50.0 ± 0.0	50.0 ± 0.0	50.0 ± 0.0	50.0 ± 0.0	50.0 ± 0.0
SphericalScore $\bar{R}_{\text{Exc}}^{(3,2)}$	87.97 ± 0.09	93.18 ± 0.55	87.2 ± 0.18	59.2 ± 0.19	65.18 ± 0.2	69.61 ± 0.23	74.24 ± 0.22	80.43 ± 0.23
SphericalScore $\bar{R}_{\text{Exc}}^{(3,1)}$	89.1 ± 0.15	93.78 ± 0.66	88.27 ± 0.2	60.54 ± 0.18	66.88 ± 0.26	71.35 ± 0.29	75.95 ± 0.29	81.88 ± 0.33
SphericalScore $\bar{R}_{\text{Exc}}^{(2,3)}$	88.0 ± 0.17	93.06 ± 0.52	87.1 ± 0.13	59.29 ± 0.11	65.18 ± 0.09	69.61 ± 0.1	74.24 ± 0.17	80.39 ± 0.21
SphericalScore $\bar{R}_{\text{Exc}}^{(2,2)}$	50.0 ± 0.0	50.0 ± 0.0	50.0 ± 0.0	50.0 ± 0.0	50.0 ± 0.0	50.0 ± 0.0	50.0 ± 0.0	50.0 ± 0.0
SphericalScore $\bar{R}_{\text{Exc}}^{(2,1)}$	89.03 ± 0.15	93.66 ± 0.64	88.2 ± 0.19	60.53 ± 0.18	66.87 ± 0.25	71.34 ± 0.29	75.93 ± 0.29	81.85 ± 0.33
SphericalScore $\bar{R}_{\text{Exc}}^{(1,3)}$	89.12 ± 0.15	93.77 ± 0.65	88.29 ± 0.2	60.54 ± 0.18	66.88 ± 0.26	71.36 ± 0.3	75.96 ± 0.29	81.89 ± 0.34
SphericalScore $\bar{R}_{\text{Exc}}^{(1,2)}$	89.17 ± 0.14	93.86 ± 0.66	88.35 ± 0.2	60.54 ± 0.18	66.88 ± 0.26	71.37 ± 0.3	75.97 ± 0.29	81.91 ± 0.34
SphericalScore $\bar{R}_{\text{Exc}}^{(1,1)}$	89.11 ± 0.15	93.77 ± 0.66	88.28 ± 0.2	60.54 ± 0.18	66.88 ± 0.26	71.36 ± 0.29	75.96 ± 0.29	81.89 ± 0.33
SphericalScore $\bar{R}_{\text{Tot}}^{(3,3)}$	90.09 ± 0.04	95.78 ± 0.64	89.4 ± 0.18	61.42 ± 0.19	68.45 ± 0.22	72.86 ± 0.26	77.3 ± 0.31	82.89 ± 0.39
SphericalScore $\bar{R}_{\text{Tot}}^{(3,2)}$	90.03 ± 0.05	95.7 ± 0.65	89.33 ± 0.18	61.42 ± 0.19	68.44 ± 0.22	72.84 ± 0.26	77.28 ± 0.31	82.86 ± 0.38
SphericalScore $\bar{R}_{\text{Tot}}^{(3,1)}$	89.82 ± 0.06	95.36 ± 0.68	89.08 ± 0.17	61.39 ± 0.19	68.4 ± 0.22	72.78 ± 0.26	77.21 ± 0.31	82.75 ± 0.38
SphericalScore $\bar{R}_{\text{Tot}}^{(2,3)}$	90.39 ± 0.03	96.2 ± 0.55	89.77 ± 0.18	61.46 ± 0.2	68.52 ± 0.23	72.94 ± 0.27	77.41 ± 0.33	83.03 ± 0.41
SphericalScore $\bar{R}_{\text{Tot}}^{(2,2)}$	90.42 ± 0.03	96.22 ± 0.54	89.81 ± 0.18	61.46 ± 0.2	68.52 ± 0.23	72.94 ± 0.28	77.41 ± 0.33	83.03 ± 0.42
SphericalScore $\bar{R}_{\text{Tot}}^{(2,1)}$	90.24 ± 0.03	96.0 ± 0.6	89.59 ± 0.18	61.44 ± 0.19	68.49 ± 0.23	72.9 ± 0.27	77.36 ± 0.32	82.96 ± 0.4
SphericalScore $\bar{R}_{\text{Tot}}^{(1,3)}$	90.39 ± 0.03	96.2 ± 0.55	89.77 ± 0.18	61.46 ± 0.2	68.52 ± 0.23	72.94 ± 0.27	77.41 ± 0.33	83.03 ± 0.41
SphericalScore $\bar{R}_{\text{Tot}}^{(1,2)}$	90.42 ± 0.03	96.22 ± 0.54	89.81 ± 0.18	61.46 ± 0.2	68.52 ± 0.23	72.94 ± 0.28	77.41 ± 0.33	83.03 ± 0.42
SphericalScore $\bar{R}_{\text{Tot}}^{(1,1)}$	90.24 ± 0.03	96.0 ± 0.6	89.59 ± 0.18	61.44 ± 0.19	68.49 ± 0.23	72.9 ± 0.27	77.36 ± 0.32	82.96 ± 0.4

1350
1351
1352
1353
1354
1355
1356
1357
1358
1359
1360
1361
1362
1363
1364
1365
1366
1367
1368
1369
1370
1371
1372
1373
1374
1375
1376
1377
1378
1379
1380
1381
1382
1383
1384
1385
1386
1387
1388
1389
1390
1391
1392
1393
1394
1395
1396
1397
1398
1399
1400
1401
1402
1403

Table 8: AUROC for out-of-distribution detection for CIFAR100 (in-distribution). As a loss function for training and for uncertainty quantification we used (Left): **Log Score**; (Middle): **Brier Score**; (Right): **Spherical Score**; Note, that due to the symmetrical nature of Brier score, many instances results to the same values.

	Log Score		BrierScore		Log Score	
	CIFAR10	SVHN	CIFAR10	SVHN	CIFAR10	SVHN
$\tilde{R}_{\text{Bayes}}^{(3)}$	77.53 ± 0.24	86.72 ± 0.53	77.18 ± 0.36	83.64 ± 0.82	77.35 ± 0.17	84.55 ± 1.36
$\tilde{R}_{\text{Bayes}}^{(2)}$	77.44 ± 0.23	86.99 ± 0.59	77.18 ± 0.36	83.64 ± 0.82	77.57 ± 0.16	84.26 ± 1.56
$\tilde{R}_{\text{Bayes}}^{(1)}$	77.3 ± 0.23	86.96 ± 0.6	76.93 ± 0.35	83.65 ± 0.97	77.39 ± 0.15	83.74 ± 1.66
$\tilde{R}_{\text{Exc}}^{(3,3)}$	50.0 ± 0.0	50.0 ± 0.0	50.0 ± 0.0	50.0 ± 0.0	50.0 ± 0.0	50.0 ± 0.0
$\tilde{R}_{\text{Exc}}^{(3,2)}$	65.33 ± 0.17	66.83 ± 1.92	50.0 ± 0.0	50.0 ± 0.0	57.9 ± 0.44	57.16 ± 2.88
$\tilde{R}_{\text{Exc}}^{(3,1)}$	72.68 ± 0.13	75.98 ± 0.72	63.26 ± 0.51	61.34 ± 1.7	66.32 ± 0.46	69.07 ± 2.06
$\tilde{R}_{\text{Exc}}^{(2,3)}$	62.97 ± 0.2	63.81 ± 2.0	50.0 ± 0.0	50.0 ± 0.0	57.11 ± 0.45	56.03 ± 2.86
$\tilde{R}_{\text{Exc}}^{(2,2)}$	50.0 ± 0.0	50.0 ± 0.0	50.0 ± 0.0	50.0 ± 0.0	50.0 ± 0.0	50.0 ± 0.0
$\tilde{R}_{\text{Exc}}^{(2,1)}$	71.35 ± 0.11	74.17 ± 0.95	63.26 ± 0.51	61.34 ± 1.7	63.94 ± 0.5	65.66 ± 2.25
$\tilde{R}_{\text{Exc}}^{(1,3)}$	71.42 ± 0.1	74.61 ± 1.06	63.26 ± 0.51	61.34 ± 1.7	64.77 ± 0.48	66.78 ± 2.23
$\tilde{R}_{\text{Exc}}^{(1,2)}$	73.2 ± 0.13	77.06 ± 0.79	63.26 ± 0.51	61.34 ± 1.7	66.97 ± 0.43	69.85 ± 2.02
$\tilde{R}_{\text{Exc}}^{(1,1)}$	72.08 ± 0.12	75.3 ± 0.88	63.26 ± 0.51	61.34 ± 1.7	65.3 ± 0.48	67.55 ± 2.18
$\tilde{R}_{\text{Tot}}^{(3,3)}$	77.53 ± 0.24	86.72 ± 0.53	77.18 ± 0.36	83.64 ± 0.82	77.35 ± 0.17	84.55 ± 1.36
$\tilde{R}_{\text{Tot}}^{(3,2)}$	77.55 ± 0.24	86.74 ± 0.52	77.18 ± 0.36	83.64 ± 0.82	77.08 ± 0.18	84.31 ± 1.29
$\tilde{R}_{\text{Tot}}^{(3,1)}$	77.5 ± 0.24	86.49 ± 0.5	76.46 ± 0.38	81.88 ± 0.48	76.78 ± 0.2	84.2 ± 1.16
$\tilde{R}_{\text{Tot}}^{(2,3)}$	77.41 ± 0.23	87.0 ± 0.58	77.18 ± 0.36	83.64 ± 0.82	77.62 ± 0.15	84.4 ± 1.53
$\tilde{R}_{\text{Tot}}^{(2,2)}$	77.44 ± 0.23	86.99 ± 0.59	77.18 ± 0.36	83.64 ± 0.82	77.57 ± 0.16	84.26 ± 1.56
$\tilde{R}_{\text{Tot}}^{(2,1)}$	77.39 ± 0.24	86.77 ± 0.55	76.46 ± 0.38	81.88 ± 0.48	77.65 ± 0.16	84.75 ± 1.44
$\tilde{R}_{\text{Tot}}^{(1,3)}$	77.41 ± 0.23	87.0 ± 0.58	77.18 ± 0.36	83.64 ± 0.82	77.62 ± 0.15	84.4 ± 1.53
$\tilde{R}_{\text{Tot}}^{(1,2)}$	77.44 ± 0.23	86.99 ± 0.59	77.18 ± 0.36	83.64 ± 0.82	77.57 ± 0.16	84.26 ± 1.56
$\tilde{R}_{\text{Tot}}^{(1,1)}$	77.39 ± 0.24	86.77 ± 0.55	76.46 ± 0.38	81.88 ± 0.48	77.65 ± 0.16	84.75 ± 1.44
$E(x; \mathbb{E}_\theta f_\theta)$	77.05 ± 0.32	87.98 ± 0.65	-	-	-	-
$\mathbb{E}_\theta E(x; f_\theta)$	76.71 ± 0.32	87.71 ± 0.69	-	-	-	-

1404
1405
1406
1407
1408
1409
1410
1411
1412
1413
1414
1415
1416
1417
1418
1419
1420
1421
1422
1423
1424
1425
1426
1427
1428
1429
1430
1431
1432
1433
1434
1435
1436
1437
1438
1439
1440
1441
1442
1443
1444
1445
1446
1447
1448
1449
1450
1451
1452
1453
1454
1455
1456
1457

Table 9: AUROC for out-of-distribution detection for TinyImageNet (in-distribution). As a loss function for training, we used **Cross-Entropy**(corresponds to Log Score). For uncertainty estimates, we used different options. From left to right: Log Score, Brier Score, Spherical Score, Zero One Score. Note, that ImageNet-O can be considered as “soft-OOD” for TinyImageNet. Note, that due to the symmetrical nature of Brier score, many instances results to the same values.

	Log Score			Spherical Score			Brier Score			Zero One Score		
	ImageNet-A	ImageNet-R	ImageNet-O	ImageNet-A	ImageNet-R	ImageNet-O	ImageNet-A	ImageNet-R	ImageNet-O	ImageNet-A	ImageNet-R	ImageNet-O
$\bar{R}_{\text{Bayes}}^{(3)}$	83.61 ± 0.2	82.67 ± 0.37	72.86 ± 0.3	83.16 ± 0.24	82.14 ± 0.34	73.3 ± 0.18	81.51 ± 0.22	80.67 ± 0.23	74.17 ± 0.22	-	-	-
$\bar{R}_{\text{Bayes}}^{(2)}$	83.76 ± 0.24	82.78 ± 0.37	73.18 ± 0.2	83.16 ± 0.24	82.14 ± 0.34	73.3 ± 0.18	83.16 ± 0.24	82.14 ± 0.34	73.3 ± 0.18	82.41 ± 0.25	81.41 ± 0.31	73.18 ± 0.16
$\bar{R}_{\text{Bayes}}^{(1)}$	83.22 ± 0.24	82.23 ± 0.39	72.21 ± 0.22	82.4 ± 0.24	81.31 ± 0.37	71.89 ± 0.17	82.68 ± 0.24	81.6 ± 0.36	72.06 ± 0.17	82.27 ± 0.23	81.2 ± 0.34	71.9 ± 0.14
$\bar{R}_{\text{Exc}}^{(3,3)}$	50.0 ± 0.0	50.0 ± 0.0	50.0 ± 0.0	50.0 ± 0.0	50.0 ± 0.0	50.0 ± 0.0	50.0 ± 0.0	50.0 ± 0.0	50.0 ± 0.0	-	-	-
$\bar{R}_{\text{Exc}}^{(3,2)}$	70.4 ± 0.45	69.75 ± 0.33	70.31 ± 0.33	50.0 ± 0.0	50.0 ± 0.0	50.0 ± 0.0	74.49 ± 0.28	74.43 ± 0.19	72.75 ± 0.3	-	-	-
$\bar{R}_{\text{Exc}}^{(3,1)}$	77.56 ± 0.28	77.02 ± 0.17	74.46 ± 0.22	65.46 ± 0.39	65.99 ± 0.37	68.81 ± 0.25	76.55 ± 0.3	76.16 ± 0.12	73.16 ± 0.22	-	-	-
$\bar{R}_{\text{Exc}}^{(2,3)}$	65.94 ± 0.44	65.34 ± 0.37	67.49 ± 0.36	50.0 ± 0.0	50.0 ± 0.0	50.0 ± 0.0	68.85 ± 0.33	69.15 ± 0.27	70.18 ± 0.28	-	-	-
$\bar{R}_{\text{Exc}}^{(2,2)}$	50.0 ± 0.0	50.0 ± 0.0	50.0 ± 0.0	50.0 ± 0.0	50.0 ± 0.0	50.0 ± 0.0	50.0 ± 0.0	50.0 ± 0.0	50.0 ± 0.0	50.0 ± 0.0	50.0 ± 0.0	50.0 ± 0.0
$\bar{R}_{\text{Exc}}^{(2,1)}$	75.94 ± 0.36	75.4 ± 0.23	74.07 ± 0.18	65.46 ± 0.39	65.99 ± 0.37	68.81 ± 0.25	70.64 ± 0.3	70.78 ± 0.23	71.04 ± 0.24	67.15 ± 0.31	67.28 ± 0.19	65.96 ± 0.33
$\bar{R}_{\text{Exc}}^{(1,3)}$	76.21 ± 0.43	75.55 ± 0.21	73.84 ± 0.17	65.46 ± 0.39	65.99 ± 0.37	68.81 ± 0.25	71.41 ± 0.3	71.46 ± 0.2	71.36 ± 0.21	-	-	-
$\bar{R}_{\text{Exc}}^{(1,2)}$	79.09 ± 0.33	78.38 ± 0.17	74.79 ± 0.25	65.46 ± 0.39	65.99 ± 0.37	68.81 ± 0.25	72.78 ± 0.28	72.67 ± 0.15	71.76 ± 0.17	70.83 ± 0.24	70.66 ± 0.13	69.13 ± 0.31
$\bar{R}_{\text{Exc}}^{(1,1)}$	77.11 ± 0.34	76.52 ± 0.19	74.46 ± 0.18	65.46 ± 0.39	65.99 ± 0.37	68.81 ± 0.25	71.9 ± 0.29	71.91 ± 0.18	71.56 ± 0.21	68.05 ± 0.32	68.21 ± 0.18	68.22 ± 0.27
$\bar{R}_{\text{Test}}^{(3,3)}$	83.61 ± 0.2	82.67 ± 0.37	72.86 ± 0.3	83.16 ± 0.24	82.14 ± 0.34	73.3 ± 0.18	81.51 ± 0.22	80.67 ± 0.23	74.17 ± 0.22	-	-	-
$\bar{R}_{\text{Test}}^{(3,2)}$	83.77 ± 0.2	82.84 ± 0.36	73.3 ± 0.27	83.16 ± 0.24	82.14 ± 0.34	73.3 ± 0.18	80.62 ± 0.24	79.92 ± 0.19	74.21 ± 0.25	-	-	-
$\bar{R}_{\text{Test}}^{(3,1)}$	83.88 ± 0.19	82.99 ± 0.32	74.09 ± 0.27	81.75 ± 0.25	81.08 ± 0.22	74.68 ± 0.27	80.47 ± 0.26	79.74 ± 0.19	74.11 ± 0.23	-	-	-
$\bar{R}_{\text{Test}}^{(2,3)}$	83.93 ± 0.24	82.95 ± 0.36	73.72 ± 0.16	83.16 ± 0.24	82.14 ± 0.34	73.3 ± 0.18	83.27 ± 0.23	82.28 ± 0.32	73.76 ± 0.19	-	-	-
$\bar{R}_{\text{Test}}^{(2,2)}$	83.76 ± 0.24	82.78 ± 0.37	73.18 ± 0.2	83.16 ± 0.24	82.14 ± 0.34	73.3 ± 0.18	83.16 ± 0.24	82.14 ± 0.34	73.3 ± 0.18	82.41 ± 0.25	81.41 ± 0.31	73.18 ± 0.16
$\bar{R}_{\text{Test}}^{(2,1)}$	84.26 ± 0.23	83.32 ± 0.31	74.93 ± 0.17	81.75 ± 0.25	81.08 ± 0.22	74.68 ± 0.27	83.25 ± 0.23	82.27 ± 0.31	73.86 ± 0.19	82.52 ± 0.23	81.56 ± 0.3	73.35 ± 0.19
$\bar{R}_{\text{Test}}^{(1,3)}$	83.93 ± 0.24	82.95 ± 0.36	73.72 ± 0.16	83.16 ± 0.24	82.14 ± 0.34	73.3 ± 0.18	83.27 ± 0.23	82.28 ± 0.32	73.76 ± 0.19	-	-	-
$\bar{R}_{\text{Test}}^{(1,2)}$	83.76 ± 0.24	82.78 ± 0.37	73.18 ± 0.2	83.16 ± 0.24	82.14 ± 0.34	73.3 ± 0.18	83.16 ± 0.24	82.14 ± 0.34	73.3 ± 0.18	82.41 ± 0.25	81.41 ± 0.31	73.18 ± 0.16
$\bar{R}_{\text{Test}}^{(1,1)}$	84.26 ± 0.23	83.32 ± 0.31	74.93 ± 0.17	81.75 ± 0.25	81.08 ± 0.22	74.68 ± 0.27	83.25 ± 0.23	82.27 ± 0.31	73.86 ± 0.19	82.52 ± 0.23	81.56 ± 0.3	73.35 ± 0.19
$E(x; E_{\theta} f_{\theta})$	83.96 ± 0.23	83.28 ± 0.41	72.72 ± 0.33	-	-	-	-	-	-	-	-	-
$E_{\theta} E(x; f_{\theta})$	82.99 ± 0.26	82.31 ± 0.45	71.15 ± 0.34	-	-	-	-	-	-	-	-	-

1458 Table 10: AUROC for misclassification detection. As a loss function for training and for uncertainty
 1459 quantification we used **Log Score**.

	CIFAR10	CIFAR100	CIFAR10-N	CIFAR100-N	TinyImageNet	
1461						
1462	LogScore $\bar{R}_{\text{Bayes}}^{(3)}$	94.76 ± 0.09	85.95 ± 0.31	80.44 ± 3.69	83.41 ± 0.23	86.55 ± 0.26
1463	LogScore $\bar{R}_{\text{Bayes}}^{(2)}$	94.7 ± 0.05	85.13 ± 0.35	78.36 ± 4.77	81.92 ± 0.36	85.5 ± 0.23
1464	LogScore $\bar{R}_{\text{Bayes}}^{(1)}$	94.39 ± 0.08	84.61 ± 0.35	78.26 ± 4.11	81.9 ± 0.29	84.99 ± 0.24
1465	LogScore $\bar{R}_{\text{Exc}}^{(3,3)}$	50.0 ± 0.0	50.0 ± 0.0	50.0 ± 0.0	50.0 ± 0.0	50.0 ± 0.0
1466	LogScore $\bar{R}_{\text{Exc}}^{(3,2)}$	92.14 ± 0.19	70.77 ± 0.38	61.28 ± 6.53	65.51 ± 0.99	71.77 ± 0.13
1467	LogScore $\bar{R}_{\text{Exc}}^{(3,1)}$	94.4 ± 0.13	82.62 ± 0.34	69.98 ± 6.08	75.51 ± 0.8	82.74 ± 0.34
1468	LogScore $\bar{R}_{\text{Exc}}^{(2,3)}$	91.54 ± 0.19	67.42 ± 0.4	59.24 ± 6.11	62.79 ± 0.97	66.83 ± 0.11
1469	LogScore $\bar{R}_{\text{Exc}}^{(2,2)}$	50.0 ± 0.0	50.0 ± 0.0	50.0 ± 0.0	50.0 ± 0.0	50.0 ± 0.0
1470	LogScore $\bar{R}_{\text{Exc}}^{(2,1)}$	94.01 ± 0.14	80.69 ± 0.35	67.7 ± 6.09	73.7 ± 0.86	80.18 ± 0.31
1471	LogScore $\bar{R}_{\text{Exc}}^{(1,3)}$	93.72 ± 0.16	80.3 ± 0.33	66.85 ± 5.94	73.37 ± 0.87	79.25 ± 0.25
1472	LogScore $\bar{R}_{\text{Exc}}^{(1,2)}$	94.23 ± 0.14	82.9 ± 0.31	69.64 ± 6.1	75.74 ± 0.78	83.22 ± 0.28
1473	LogScore $\bar{R}_{\text{Exc}}^{(1,1)}$	94.1 ± 0.14	81.58 ± 0.34	68.39 ± 6.07	74.52 ± 0.83	81.33 ± 0.29
1474	LogScore $\bar{R}_{\text{Tot}}^{(3,3)}$	94.76 ± 0.09	85.95 ± 0.31	80.44 ± 3.69	83.41 ± 0.23	86.55 ± 0.26
1475	LogScore $\bar{R}_{\text{Tot}}^{(3,2)}$	94.77 ± 0.05	85.96 ± 0.32	80.21 ± 3.96	83.33 ± 0.26	86.5 ± 0.25
1476	LogScore $\bar{R}_{\text{Tot}}^{(3,1)}$	94.74 ± 0.07	86.22 ± 0.31	79.38 ± 3.85	83.18 ± 0.29	86.65 ± 0.26
1477	LogScore $\bar{R}_{\text{Tot}}^{(2,3)}$	94.4 ± 0.06	85.01 ± 0.37	76.26 ± 5.04	81.67 ± 0.39	85.18 ± 0.23
1478	LogScore $\bar{R}_{\text{Tot}}^{(2,2)}$	94.01 ± 0.05	85.13 ± 0.35	78.36 ± 4.77	81.92 ± 0.36	85.5 ± 0.23
1479	LogScore $\bar{R}_{\text{Tot}}^{(2,1)}$	94.5 ± 0.06	85.43 ± 0.35	75.73 ± 4.68	81.67 ± 0.41	85.58 ± 0.22
1480	LogScore $\bar{R}_{\text{Tot}}^{(1,3)}$	94.4 ± 0.06	85.01 ± 0.37	76.26 ± 5.04	81.67 ± 0.39	85.18 ± 0.23
1481	LogScore $\bar{R}_{\text{Tot}}^{(1,2)}$	94.7 ± 0.05	85.13 ± 0.35	78.36 ± 4.77	81.92 ± 0.36	85.5 ± 0.23
1482	LogScore $\bar{R}_{\text{Tot}}^{(1,1)}$	94.5 ± 0.06	85.43 ± 0.35	75.73 ± 4.68	81.67 ± 0.41	85.58 ± 0.22
1483	LogScore $E(x; \mathbb{E}_\theta f_\theta)$	93.89 ± 0.11	82.95 ± 0.34	74.82 ± 5.48	76.74 ± 0.64	83.34 ± 0.23
1484	LogScore $\mathbb{E}_\theta E(x; f_\theta)$	93.38 ± 0.15	82.07 ± 0.34	74.61 ± 5.23	76.12 ± 0.63	82.4 ± 0.24

1483 K ADDITIONAL EXPERIMENTS ON MISCLASSIFICATION DETECTION

1484 In this section, we present additional results for misclassification detection.

1485 As training datasets, we consider CIFAR10, CIFAR100, their noisy versions as well as TinyImageNet
 1486 (only with Cross-Entropy loss function).

1487 In Table 10 we present results for all these datasets, when loss function and instantiation are generated
 1488 by Log Score. In Tables 11 and 12, we present results for CIFAR-like datasets, as for TinyImageNet
 1489 we have only Cross-Entropy loss function. From all these tables we see that, indeed, Bayes risk and
 1490 Total risk are the best choices when encounter misclassification detection problem. The gap is even
 1491 more significant, when more label noise is introduced. Moreover, instantiations for Log Score are
 1492 typically provide better AUROC, than others. Similarly to the out-of-distribution detection, it justifies
 1493 typical practical choice for Log Score-based measures.

1494 For TinyImageNet, results are presented in Table 13. Similarly to Table 9, one loss function was used
 1495 for training, while different instantiations of G were used for the measures of uncertainty. Interestingly,
 1496 the best results are reached by Zero One score, that is also a popular choice of practitioners.

1512
1513
1514
1515
1516
1517
1518
1519
1520
1521
1522
1523
1524
1525
1526
1527
1528
1529
1530
1531
1532
1533
1534
1535
1536
1537
1538
1539
1540
1541
1542
1543
1544
1545
1546
1547
1548
1549
1550
1551
1552
1553
1554
1555
1556
1557
1558
1559
1560
1561
1562
1563
1564
1565

Table 11: AUROC for misclassification detection. As a loss function for training and for uncertainty quantification we used **Brier Score**. Note, that due to the symmetrical nature of Brier score, many instances results to the same values.

	CIFAR10	CIFAR100	CIFAR10-N	CIFAR100-N
BrierScore $\tilde{R}_{\text{Bayes}}^{(3)}$	94.68 ± 0.3	86.02 ± 0.26	80.64 ± 3.17	84.1 ± 0.13
BrierScore $\tilde{R}_{\text{Bayes}}^{(2)}$	94.68 ± 0.3	86.02 ± 0.26	80.64 ± 3.17	84.1 ± 0.13
BrierScore $\tilde{R}_{\text{Bayes}}^{(1)}$	94.22 ± 0.27	85.09 ± 0.27	79.2 ± 2.35	83.95 ± 0.14
BrierScore $\tilde{R}_{\text{Exc}}^{(3,3)}$	50.0 ± 0.0	50.0 ± 0.0	50.0 ± 0.0	50.0 ± 0.0
BrierScore $\tilde{R}_{\text{Exc}}^{(3,2)}$	50.0 ± 0.0	50.0 ± 0.0	50.0 ± 0.0	50.0 ± 0.0
BrierScore $\tilde{R}_{\text{Exc}}^{(3,1)}$	94.2 ± 0.34	72.71 ± 0.34	76.31 ± 3.39	65.34 ± 0.43
BrierScore $\tilde{R}_{\text{Exc}}^{(2,3)}$	50.0 ± 0.0	50.0 ± 0.0	50.0 ± 0.0	50.0 ± 0.0
BrierScore $\tilde{R}_{\text{Exc}}^{(2,2)}$	50.0 ± 0.0	50.0 ± 0.0	50.0 ± 0.0	50.0 ± 0.0
BrierScore $\tilde{R}_{\text{Exc}}^{(2,1)}$	94.2 ± 0.34	72.71 ± 0.34	76.31 ± 3.39	65.34 ± 0.43
BrierScore $\tilde{R}_{\text{Exc}}^{(1,3)}$	94.2 ± 0.34	72.71 ± 0.34	76.31 ± 3.39	65.34 ± 0.43
BrierScore $\tilde{R}_{\text{Exc}}^{(1,2)}$	94.2 ± 0.34	72.71 ± 0.34	76.31 ± 3.39	65.34 ± 0.43
BrierScore $\tilde{R}_{\text{Exc}}^{(1,1)}$	94.2 ± 0.34	72.71 ± 0.34	76.31 ± 3.39	65.34 ± 0.43
BrierScore $\tilde{R}_{\text{Tot}}^{(3,3)}$	94.68 ± 0.3	86.02 ± 0.26	80.64 ± 3.17	84.1 ± 0.13
BrierScore $\tilde{R}_{\text{Tot}}^{(3,2)}$	94.68 ± 0.3	86.02 ± 0.26	80.64 ± 3.17	84.1 ± 0.13
BrierScore $\tilde{R}_{\text{Tot}}^{(3,1)}$	94.61 ± 0.31	86.11 ± 0.23	79.78 ± 3.23	83.24 ± 0.19
BrierScore $\tilde{R}_{\text{Tot}}^{(2,3)}$	94.68 ± 0.3	86.02 ± 0.26	80.64 ± 3.17	84.1 ± 0.13
BrierScore $\tilde{R}_{\text{Tot}}^{(2,2)}$	94.68 ± 0.3	86.02 ± 0.26	80.64 ± 3.17	84.1 ± 0.13
BrierScore $\tilde{R}_{\text{Tot}}^{(2,1)}$	94.61 ± 0.31	86.11 ± 0.23	79.78 ± 3.23	83.24 ± 0.19
BrierScore $\tilde{R}_{\text{Tot}}^{(1,3)}$	94.68 ± 0.3	86.02 ± 0.26	80.64 ± 3.17	84.1 ± 0.13
BrierScore $\tilde{R}_{\text{Tot}}^{(1,2)}$	94.68 ± 0.3	86.02 ± 0.26	80.64 ± 3.17	84.1 ± 0.13
BrierScore $\tilde{R}_{\text{Tot}}^{(1,1)}$	94.61 ± 0.31	86.11 ± 0.23	79.78 ± 3.23	83.24 ± 0.19

Table 12: AUROC for misclassification detection. As a loss function for training and for uncertainty quantification we used **Spherical Score**.

	CIFAR10	CIFAR100	CIFAR10-N	CIFAR100-N
SphericalScore $\tilde{R}_{\text{Bayes}}^{(3)}$	94.01 ± 0.31	85.37 ± 0.25	79.36 ± 2.85	80.13 ± 0.6
SphericalScore $\tilde{R}_{\text{Bayes}}^{(2)}$	94.15 ± 0.29	84.73 ± 0.24	80.8 ± 3.0	80.53 ± 0.54
SphericalScore $\tilde{R}_{\text{Bayes}}^{(1)}$	93.64 ± 0.28	83.97 ± 0.25	80.35 ± 3.11	80.03 ± 0.52
SphericalScore $\tilde{R}_{\text{Exc}}^{(3,3)}$	50.0 ± 0.0	50.0 ± 0.0	50.0 ± 0.0	50.0 ± 0.0
SphericalScore $\tilde{R}_{\text{Exc}}^{(3,2)}$	92.81 ± 0.49	65.29 ± 0.48	69.95 ± 5.62	61.62 ± 0.33
SphericalScore $\tilde{R}_{\text{Exc}}^{(3,1)}$	93.46 ± 0.47	77.3 ± 0.35	75.18 ± 3.6	71.81 ± 0.46
SphericalScore $\tilde{R}_{\text{Exc}}^{(2,3)}$	92.76 ± 0.41	64.33 ± 0.47	70.03 ± 5.53	60.8 ± 0.32
SphericalScore $\tilde{R}_{\text{Exc}}^{(2,2)}$	50.0 ± 0.0	50.0 ± 0.0	50.0 ± 0.0	50.0 ± 0.0
SphericalScore $\tilde{R}_{\text{Exc}}^{(2,1)}$	93.39 ± 0.47	73.76 ± 0.36	75.06 ± 3.53	68.84 ± 0.42
SphericalScore $\tilde{R}_{\text{Exc}}^{(1,3)}$	93.51 ± 0.47	75.08 ± 0.36	75.22 ± 3.63	69.97 ± 0.42
SphericalScore $\tilde{R}_{\text{Exc}}^{(1,2)}$	93.57 ± 0.46	78.25 ± 0.34	75.32 ± 3.69	72.69 ± 0.44
SphericalScore $\tilde{R}_{\text{Exc}}^{(1,1)}$	93.49 ± 0.47	75.83 ± 0.35	75.2 ± 3.61	70.59 ± 0.43
SphericalScore $\tilde{R}_{\text{Tot}}^{(3,3)}$	94.01 ± 0.31	85.37 ± 0.25	79.36 ± 2.85	80.13 ± 0.6
SphericalScore $\tilde{R}_{\text{Tot}}^{(3,2)}$	93.98 ± 0.31	85.16 ± 0.24	79.29 ± 2.84	79.95 ± 0.6
SphericalScore $\tilde{R}_{\text{Tot}}^{(3,1)}$	93.92 ± 0.31	85.42 ± 0.24	79.21 ± 2.79	80.13 ± 0.61
SphericalScore $\tilde{R}_{\text{Tot}}^{(2,3)}$	94.15 ± 0.29	84.88 ± 0.24	80.66 ± 3.03	80.6 ± 0.54
SphericalScore $\tilde{R}_{\text{Tot}}^{(2,2)}$	94.15 ± 0.29	84.73 ± 0.24	80.8 ± 3.0	80.53 ± 0.54
SphericalScore $\tilde{R}_{\text{Tot}}^{(2,1)}$	94.14 ± 0.3	85.23 ± 0.23	80.15 ± 2.99	80.82 ± 0.55
SphericalScore $\tilde{R}_{\text{Tot}}^{(1,3)}$	94.15 ± 0.29	84.88 ± 0.24	80.66 ± 3.03	80.6 ± 0.54
SphericalScore $\tilde{R}_{\text{Tot}}^{(1,2)}$	94.15 ± 0.29	84.73 ± 0.24	80.8 ± 3.0	80.53 ± 0.54
SphericalScore $\tilde{R}_{\text{Tot}}^{(1,1)}$	94.14 ± 0.3	85.23 ± 0.23	80.15 ± 2.99	80.82 ± 0.55

1566
1567
1568
1569
1570
1571
1572
1573
1574
1575
1576
1577
1578
1579
1580
1581
1582
1583
1584
1585
1586
1587
1588
1589
1590
1591
1592
1593
1594
1595
1596
1597
1598
1599
1600
1601
1602
1603
1604
1605
1606
1607
1608
1609
1610
1611
1612
1613
1614
1615
1616
1617
1618
1619

Table 13: AUROC for misclassification detection (TinyImageNet). As a loss function for training we used Cross-Entropy. Here, we try different instantiations of G for uncertainty measures. Note, that due to the symmetrical nature of Brier score, many instances results to the same values.

	Log Score	Brier Score	Spherical Score	Zero One Score
$\tilde{R}_{\text{Bayes}}^{(3)}$	86.55 ± 0.26	86.8 ± 0.28	85.83 ± 0.36	-
$\tilde{R}_{\text{Bayes}}^{(2)}$	85.5 ± 0.23	86.8 ± 0.28	86.8 ± 0.28	87.23 ± 0.35
$\tilde{R}_{\text{Bayes}}^{(1)}$	84.99 ± 0.24	85.89 ± 0.27	85.76 ± 0.26	85.88 ± 0.27
$\tilde{R}_{\text{Exc}}^{(3,3)}$	50.0 ± 0.0	50.0 ± 0.0	50.0 ± 0.0	-
$\tilde{R}_{\text{Exc}}^{(3,2)}$	71.77 ± 0.13	50.0 ± 0.0	81.82 ± 0.47	-
$\tilde{R}_{\text{Exc}}^{(3,1)}$	82.74 ± 0.34	75.91 ± 0.59	83.6 ± 0.47	-
$\tilde{R}_{\text{Exc}}^{(2,3)}$	66.83 ± 0.11	50.0 ± 0.0	78.32 ± 0.58	-
$\tilde{R}_{\text{Exc}}^{(2,2)}$	50.0 ± 0.0	50.0 ± 0.0	50.0 ± 0.0	50.0 ± 0.0
$\tilde{R}_{\text{Exc}}^{(2,1)}$	80.18 ± 0.31	75.91 ± 0.59	79.62 ± 0.54	73.59 ± 0.44
$\tilde{R}_{\text{Exc}}^{(1,3)}$	79.25 ± 0.25	75.91 ± 0.59	80.73 ± 0.54	-
$\tilde{R}_{\text{Exc}}^{(1,2)}$	83.22 ± 0.28	75.91 ± 0.59	81.95 ± 0.55	79.52 ± 0.68
$\tilde{R}_{\text{Exc}}^{(1,1)}$	81.33 ± 0.29	75.91 ± 0.59	81.02 ± 0.54	76.78 ± 0.56
$\tilde{R}_{\text{Tot}}^{(3,3)}$	86.55 ± 0.26	86.8 ± 0.28	85.83 ± 0.36	-
$\tilde{R}_{\text{Tot}}^{(3,2)}$	86.5 ± 0.25	86.8 ± 0.28	85.39 ± 0.37	-
$\tilde{R}_{\text{Tot}}^{(3,1)}$	86.65 ± 0.26	86.4 ± 0.32	85.43 ± 0.39	-
$\tilde{R}_{\text{Tot}}^{(2,3)}$	85.18 ± 0.23	86.8 ± 0.28	86.9 ± 0.29	-
$\tilde{R}_{\text{Tot}}^{(2,2)}$	85.5 ± 0.23	86.8 ± 0.28	86.8 ± 0.28	87.23 ± 0.35
$\tilde{R}_{\text{Tot}}^{(2,1)}$	85.58 ± 0.22	86.4 ± 0.32	86.92 ± 0.3	86.95 ± 0.31
$\tilde{R}_{\text{Tot}}^{(1,3)}$	85.18 ± 0.23	86.8 ± 0.28	86.9 ± 0.29	-
$\tilde{R}_{\text{Tot}}^{(1,2)}$	85.5 ± 0.23	86.8 ± 0.28	86.8 ± 0.28	87.23 ± 0.35
$\tilde{R}_{\text{Tot}}^{(1,1)}$	85.58 ± 0.22	86.4 ± 0.32	86.92 ± 0.3	86.95 ± 0.31
$E(x; \mathbb{E}_\theta f_\theta)$	83.34 ± 0.23	-	-	-
$\mathbb{E}_\theta E(x; f_\theta)$	82.4 ± 0.24	-	-	-

L DERIVATION OF CENTRAL PREDICTIONS

Central prediction is defined as $\bar{\eta} = \arg \min_z \mathbb{E}_\theta D_G(z \parallel \eta_\theta)$. For different instantiations of G , there will be different central predictions. In what follows, we will abuse the subscription θ , and simply write \mathbb{E} and η , assuming expectation with respect to θ .

Recall, that Bregman divergence is:

$$D_G(z \parallel \eta) = G(z) - G(\eta) - \langle G'(\eta), z - \eta \rangle$$

L.1 LOGSCORE

$$G(\eta) = \sum_{k=1}^K \eta_k \log \eta_k,$$

$$G'(\eta)_k = 1 + \log \eta_k,$$

$$\begin{aligned} \bar{\eta} &= \arg \min_z \left[\sum_k z_k \log z_k - \mathbb{E} \sum_k \eta_k \log \eta_k - \langle 1 + \mathbb{E} \log \eta, z \rangle + \mathbb{E} \langle 1 + \log \eta, \eta \rangle \right] = \\ &= \arg \min_z \left[\sum_k z_k \log z_k - \mathbb{E} \sum_k \eta_k \log \eta_k - \sum_k z_k \log (\exp \mathbb{E} \log \eta)_k + \mathbb{E} \sum_k \eta_k \log \eta_k \right] = \\ &= \arg \min_z \left[\sum_k z_k \log z_k - \sum_k z_k \log (\exp \mathbb{E} \log \eta)_k \right] = \\ &= \arg \min_z \left[\sum_k z_k \log z_k - \sum_k z_k \log (\exp \mathbb{E} \log \eta)_k - \right. \\ &\quad \left. \sum_k z_k \sum_{k'} \log (\exp \mathbb{E} \log \eta)_{k'} + \sum_k z_k \sum_{k'} \log (\exp \mathbb{E} \log \eta)_{k'} \right] = \\ &= \arg \min_z \left[\sum_k z_k \log z_k - \sum_k z_k \log \frac{(\exp \mathbb{E} \log \eta)_k}{\sum_{k'} (\exp \mathbb{E} \log \eta)_{k'}} \right] = \\ &= \arg \min_z \left[\text{KL}(z \parallel \frac{(\exp \mathbb{E} \log \eta)_k}{\sum_{k'} (\exp \mathbb{E} \log \eta)_{k'}}) \right], \end{aligned}$$

hence, $\bar{\eta}_k = \frac{(\exp \mathbb{E} \log \eta)_k}{\sum_{k'} (\exp \mathbb{E} \log \eta)_{k'}}$.

L.2 BRIER SCORE

$$G(\eta) = - \sum_{k=1}^K \eta_k (1 - \eta_k),$$

$$G'(\eta)_k = 2\eta_k - 1,$$

1674

1675

1676

1677

1678

1679

1680

1681

1682

1683

1684

1685

1686

1687

1688

1689

1690

1691

1692

1693

1694

1695

1696

1697

1698

1699

1700

1701

1702

1703

1704

1705

1706

1707

1708

1709

1710

1711

1712

1713

1714

1715

1716

1717

1718

1719

1720

1721

1722

1723

1724

1725

1726

1727

$$\begin{aligned}
\bar{\eta} &= \arg \min_z \left[-\sum_k z_k(1-z_k) + \mathbb{E} \sum_k \eta_k(1-\eta_k) - \langle 2\mathbb{E}\eta - 1, z \rangle + \mathbb{E} \langle 2\eta - 1, \eta \rangle \right] = \\
& \arg \min_z \left[-\sum_k z_k(1-z_k) + \mathbb{E} \sum_k \eta_k(1-\eta_k) - 2 \sum_k z_k \mathbb{E} \eta_k + 2\mathbb{E} \sum_k \eta_k^2 \right] = \\
& \arg \min_z \left[\sum_k z_k^2 - \mathbb{E} \sum_k \eta_k^2 - 2 \sum_k z_k \mathbb{E} \eta_k + 2\mathbb{E} \sum_k \eta_k^2 \right] = \\
& = \arg \min_z \left[\sum_k z_k^2 - 2 \sum_k z_k \mathbb{E} \eta_k + \mathbb{E} \sum_k \eta_k^2 \right] = \\
& \arg \min_z \left[\sum_k z_k^2 - 2 \sum_k z_k \mathbb{E} \eta_k + \mathbb{E} \sum_k \eta_k^2 + \sum_k (\mathbb{E} \eta_k)^2 - \sum_k (\mathbb{E} \eta_k)^2 \right] = \\
& \arg \min_z \left[\|z - \mathbb{E}\eta\|_2^2 + \mathbb{E} \sum_k \eta_k^2 - \sum_k (\mathbb{E} \eta_k)^2 \right] = \\
& \arg \min_z \left[\|z - \mathbb{E}\eta\|_2^2 \right],
\end{aligned}$$

hence, $\bar{\eta} = \mathbb{E}\eta$.

L.3 ZERO-ONE SCORE

$$G(\eta) = \max_k \eta_k - 1,$$

$$G'(\eta)_k = \mathbb{I}[k = \arg \max_j \eta_j],$$

$$\begin{aligned}
\bar{\eta} &= \arg \min_z \mathbb{E} \left[\max_k z_k - 1 - \max_k \eta_k + 1 - \langle \mathbb{I}[\arg \max_j \eta_j], z - \eta \rangle \right] = \\
& \arg \min_z \mathbb{E} \left[\max_k z_k - \max_k \eta_k - (z - \eta)_{\arg \max_j \eta_j} \right] = \arg \min_z \mathbb{E} \left[\max_k z_k - z_{\arg \max_j \eta_j} \right] = \\
& \arg \min_z \left[\max_k z_k - \langle z, \mathbb{E} \mathbb{I}[\arg \max_j \eta_j] \rangle \right] = \arg \min_z \left[\max_k z_k - \langle z, \tilde{p} \rangle \right] = \\
& \arg \min_z \langle z, \mathbb{I}[\arg \max_j \eta_j] - \tilde{p} \rangle = 0
\end{aligned}$$

where $\tilde{p} = \mathbb{E} \mathbb{I}[\arg \max_j \eta_j]$ are empirical frequencies of class labels, predicted by models, parametrized by samples from $p(\theta | D_{tr})$.

We can see, that minimum is always reached with $\bar{\eta} = \text{Uniform}(K)$, where $\text{Uniform}(K)$ is a uniform categorical distribution over K classes. Please note, that there might be infinitely many solutions, when at least one of the components of \tilde{p} is 0.

Let us assume that there are no zero components, hence uniform distribution will be the only solution.

However, uniform distribution plug-in violates general decomposition in equation (11).

This might be due to the requirement, that G must be a strictly convex, while $G(\eta) = \max_k \eta_k - 1$ is only convex, and effectively operates with the single (maximal) component of the categorical distribution η , while undetermine others.

L.4 SPHERICAL SCORE

$$G(\eta) = \|\eta\|_2 - 1$$

$$G'(\eta)_k = \frac{\eta_k}{\|\eta\|_2}$$

1728
1729
1730
1731
1732
1733
1734

$$\begin{aligned}\bar{\eta} &= \arg \min_z \mathbb{E} \left[\|z\|_2 - \|\eta\|_2 + \left\langle \frac{\eta}{\|\eta\|_2}, \eta - z \right\rangle \right] \\ &= \arg \min_z \mathbb{E} \left[\|z\|_2 - \left\langle \frac{\eta}{\|\eta\|_2}, z \right\rangle \right] \\ &= \arg \min_z \|z\|_2 - \langle z, \mathbb{E} \left[\frac{\eta}{\|\eta\|_2} \right] \rangle\end{aligned}$$

1735

Lets introduce following notation:

1736

1737

1738

1739

1740

1741

1742

1743

1744

1745

1746

$$\begin{aligned}f(z, \eta) &= \arg \min_z \|z\|_2 - \langle z, \mathbb{E} \left[\frac{\eta}{\|\eta\|_2} \right] \rangle \\ \eta_E &= \mathbb{E} \left[\frac{\eta}{\|\eta\|_2} \right] \\ x_0 &= \left(\frac{1}{K}, \dots, \frac{1}{K} \right) \in \mathbb{R}^K \\ x_{\parallel} &:= x_{\parallel} \in \mathbb{R}^K \text{ s.t. } x_{\parallel} \parallel x_0 \\ x_{\perp} &:= x_{\perp} \in \mathbb{R}^K \text{ s.t. } x_{\perp} \perp x_0, \|x_{\perp}\| = 1 \\ a &:= a \in \mathbb{R}^K \text{ s.t. } a \perp x_0, a \perp x_{\perp}, \|a\|_2 = 1.\end{aligned}$$

1747

Then we can say, that there exists k_{η}, k, k_a such that:

1748

1749

1750

1751

1752

1753

1754

1755

1756

1757

1758

$$\begin{aligned}\eta_E &= x_{\parallel} + k_{\eta} x_{\perp}, \quad z = x_0 + k x_{\perp} + k_a a, \\ f(k_{\eta}, k, k_a) &= \|x_0 + k x_{\perp} + k_a a\|_2 \\ &\quad - \langle x_0 + k x_{\perp} + k_a a, x_{\parallel} + k_{\eta} x_{\perp} \rangle \\ &= \sqrt{\sum_i (x_0)_i^2 + k^2 \sum_i (x_{\perp})_i^2 + k_a^2 \sum_i a_i^2} \\ &\quad - (k_{\eta} k + \langle x_0, x_{\parallel} \rangle) \\ &= \sqrt{\sum_i (x_0)_i^2 + k^2 + k_a^2} - k_{\eta} k - \langle x_0, x_{\parallel} \rangle.\end{aligned}$$

1759

1760

Lets takes derivatives of $f(\cdot)$ w.r.t k, k_a to find values, that minimize it:

1761

1762

1763

1764

1765

1766

1767

1768

1769

1770

1771

1772

1773

1774

1775

1776

1777

1778

1779

1780

1781

$$\begin{aligned}\frac{df(k_{\eta}, k, k_a)}{dk_a} &= \frac{k_a}{\sqrt{\sum_i (x_0)_i^2 + k^2 + k_a^2}} = 0 \\ \sum_i (x_0)_i^2 + k^2 \neq 0 &\implies k_a = 0\end{aligned}$$

$$\begin{aligned}\frac{df(k_{\eta}, k, k_a)}{dk} &= \frac{k}{\sqrt{\sum_i (x_0)_i^2 + k^2}} - k_{\eta} = 0 \\ k^2 &= k_{\eta}^2 (\sum_i (x_0)_i^2 + k^2)\end{aligned}$$

$$k^2 (1 - k_{\eta}^2) = k_{\eta}^2 \|x_0\|_2^2 \implies k = \frac{k_{\eta} \|x_0\|_2}{\sqrt{1 - k_{\eta}^2}}$$

$$x_{\parallel} = \langle \eta_E, x_0 \rangle \frac{x_0}{\|x_0\|_2^2}$$

$$\begin{aligned}k_{\eta} &= k_{\eta} \|x_{\perp}\|_2 = \|\eta_E - x_{\parallel}\|_2^2 \\ &= \|\eta_E - \langle \eta_E, x_0 \rangle \frac{x_0}{\|x_0\|_2^2}\|_2.\end{aligned}$$

1782 Finally we have:

$$\begin{aligned}
1783 & z = x_0 + kx_{\perp} + k_a a \\
1784 & \\
1785 & = x_0 + \frac{k}{k_{\eta}}(\eta_E - x_{\parallel}) = x_0 + \frac{\eta_E - x_{\parallel}}{\sqrt{1 - k_{\eta}^2}} \|x_0\|_2 \\
1786 & \\
1787 & \\
1788 & = x_0 + \frac{\eta_E - \langle \eta_E, x_0 \rangle \frac{x_0}{\|x_0\|_2^2}}{\sqrt{1 - \|\eta_E - \langle \eta_E, x_0 \rangle \frac{x_0}{\|x_0\|_2^2}\|_2^2}} \|x_0\|_2. \\
1789 & \\
1790 &
\end{aligned}$$

1791 Setting $n = \frac{x_0}{\|x_0\|}$ and $m = \eta_E - \langle \eta_E, x_0 \rangle \frac{x_0}{\|x_0\|_2^2}$ we conclude:

$$1793 \quad z = \|x_0\|_2 \left[n + \frac{m}{\sqrt{1 - \|m\|_2^2}} \right].$$

1796 M TOY EXAMPLE

1797 In this section, we consider a specific toy example, in which uncertainty measures can be computed
1798 in closed form.

1801 Specifically, we consider the problem of binary classification, where the likelihood (predictive model)
1802 is simply a Bernoulli distribution, and the prior distribution over model parameter (the probability of
1803 success) is Beta distribution. Therefore, prior and likelihood are conjugate, and the posterior is Beta
1804 distribution as well.

1805 **Expected Pairwise Kullback–Leibler (EPKL).** Here, we want to estimate

$$\begin{aligned}
1807 & \mathbb{E}_{\theta^*} \mathbb{E}_{\theta} KL(\theta^* \| \theta) = \\
1808 & \mathbb{E}_{\theta^*} [\theta^* \log \theta^*] - \mathbb{E}_{\theta^*} [\theta^*] \mathbb{E}_{\theta} [\log \theta] + \mathbb{E}_{\theta^*} [(1 - \theta^*) \log(1 - \theta^*)] - \mathbb{E}_{\theta^*} [(1 - \theta^*)] \mathbb{E}_{\theta} [\log(1 - \theta)].
\end{aligned}$$

1810 We assume that $p(\theta^* | D) = \text{Beta}(\alpha^*, \beta^*)$, and $p(\theta | D) = \text{Beta}(\alpha, \beta)$. Each of the components can
1811 be computed analytically:

- 1813 1. $\mathbb{E}_{\theta^*} [\theta^* \log \theta^*] = \frac{\alpha^*}{\alpha^* + \beta^*} [\psi(\alpha^* + 1) - \psi(\alpha^* + \beta^* + 1)];$
- 1814 2. $\mathbb{E}_{\theta^*} \theta^* = \frac{\alpha^*}{\alpha^* + \beta^*};$
- 1815 3. $\mathbb{E}_{\theta} \log \theta = \psi(\alpha) - \psi(\alpha + \beta);$
- 1816 4. $\mathbb{E}_{\theta^*} [(1 - \theta^*) \log(1 - \theta^*)] = \frac{\beta^*}{\alpha^* + \beta^*} [\psi(\beta^* + 1) - \psi(\alpha^* + \beta^* + 1)];$
- 1817 5. $\mathbb{E}_{\theta^*} (1 - \theta^*) = \frac{\beta^*}{\alpha^* + \beta^*};$
- 1818 6. $\mathbb{E}_{\theta} [\log(1 - \theta)] = \psi(\beta) - \psi(\alpha + \beta).$

1819 If we assume, that $\alpha^* = \alpha$ and $\beta^* = \beta$ (the setup we considered in the main part), then one can show,
1820 using these six equations that

$$1821 \quad \text{EPKL} = \frac{1}{\alpha + \beta}.$$

1822 Note, that this assumption (on the equal parameters) was done for simplicity. In general case, one can
1823 indeed consider different Bayesian models for the approximation of the ground truth distribution and
1824 for the approximation of the prediction. But since it is done at the cost of training a separate Bayesian
1825 model, we believe it might be not of a big practical value.

1826 **Mutual Information (MI).** Following the derivations from the main part, MI can be represented
1827 as:

$$\begin{aligned}
1828 & \mathbb{E}_{\theta} KL(\theta^* \| \mathbb{E}_{\theta} \theta) = \\
1829 & \mathbb{E}_{\theta^*} [\theta^* \log \theta^*] - \mathbb{E}_{\theta^*} [\theta^*] \log \mathbb{E}_{\theta} \theta + \mathbb{E}_{\theta^*} [(1 - \theta^*) \log(1 - \theta^*)] - \mathbb{E}_{\theta^*} [(1 - \theta^*)] \log(1 - \mathbb{E}_{\theta} \theta).
\end{aligned}$$

Again, we use the same assumption on the equal parameters of the posterior distributions. With the equations from the above, we obtain:

$$\text{MI} = \frac{1}{\alpha + \beta} + \frac{\alpha}{\alpha + \beta} [\psi(\alpha) - \psi(\alpha + \beta) - \log \alpha] + \frac{\beta}{\alpha + \beta} [\psi(\beta) - \psi(\alpha + \beta) - \log \beta] + \log(\alpha + \beta).$$

Reverse Mutual Information (RMI). As we showed in the main part, RMI can be presented as follows:

$$\mathbb{E}_{\theta} KL(\mathbb{E}_{\theta^*} \theta^* || \theta) = \mathbb{E}_{\theta^*} [\theta^*] [\log \mathbb{E}_{\theta^*} \theta^*] - \mathbb{E}_{\theta^*} [\theta^*] \mathbb{E}_{\theta} [\log \theta] + (1 - \mathbb{E}_{\theta^*} \theta^*) \log(1 - \mathbb{E}_{\theta^*} \theta^*) - (1 - \mathbb{E}_{\theta^*} \theta^*) \mathbb{E}_{\theta} [\log(1 - \theta)].$$

Following the same methodology as for previous cases, we obtain:

$$\text{RMI} = \frac{\alpha}{\alpha + \beta} (\log \alpha - \psi(\alpha) + \psi(\alpha + \beta)) + \frac{\beta}{\alpha + \beta} (\log \beta - \psi(\beta) + \psi(\alpha + \beta)) - \log(\alpha + \beta).$$

It is easy to see, that EPKL = MI + RMI (which is consistent with the general result that $\tilde{\mathbf{R}}_{\text{Exc}}^{(1,1)} = \tilde{\mathbf{R}}_{\text{Exc}}^{(1,2)} + \tilde{\mathbf{R}}_{\text{Exc}}^{(2,1)}$).

Expected Pairwise Brier Score (EPBS). In this case, we would like to estimate the following quantity:

$$\mathbb{E}_{\theta^*} \mathbb{E}(\theta^* - \theta)^2 = \mathbb{E}_{\theta^*} [\theta^*]^2 - 2\mathbb{E}_{\theta^*} [\theta^*] \mathbb{E}_{\theta} [\theta] + \mathbb{E}_{\theta} [\theta]^2.$$

If we assume, that the parameters of the posterior distributions are equal, then the whole equation above reduces to the double variance of θ . In case of Beta distribution, it equals to:

$$\text{EPBS} = 2\text{var}\theta = \frac{2\alpha\beta}{(\alpha + \beta)^2(\alpha + \beta + 1)}.$$

Note, that the posterior update rule for this simple Beta-Bernoulli model is:

$$\alpha = \alpha_{\text{prior}} + x,$$

and

$$\beta = \beta_{\text{prior}} + n - x,$$

where by subscript ‘‘prior’’ we highlight the parameters of the prior distribution, x is the number of successes in observed training dataset, and n is the total number of observations.

Therefore we see, that given larger θ training dataset, the estimates of epistemic uncertainty will shrink. This is the property we typically want to have from the epistemic uncertainty estimates – the bigger the dataset, the less uncertainty.

However, in case of the prior misspecification (will be discussed below), it leads to certain problems. If the prior parameters α_{prior} and β_{prior} are already large (indicating a highly concentrated prior), the posterior will also be highly concentrated, regardless of the data. This can lead to an underestimation of epistemic uncertainty because the model appears more certain than it should be.

M.1 VARIOUS DISTRIBUTION SHAPES

In this section, we explore different choices of the parameters and demonstrate, how the resulting posterior distribution will look like, given different prior and different sizes of training datasets. We show the resulting plots at the Figure 4. Note, that as a ground-truth we used $\theta^* = 0.9$. We see, that given enough data, the mass of the posterior is concentrated around the correct value of the parameter, regardless of the prior misspecification.

1890
 1891
 1892
 1893
 1894
 1895
 1896
 1897
 1898
 1899
 1900
 1901
 1902
 1903
 1904
 1905
 1906
 1907
 1908
 1909
 1910
 1911
 1912
 1913
 1914
 1915
 1916
 1917
 1918
 1919
 1920
 1921
 1922
 1923
 1924
 1925
 1926
 1927
 1928
 1929
 1930
 1931
 1932
 1933
 1934
 1935
 1936
 1937
 1938
 1939
 1940
 1941
 1942
 1943

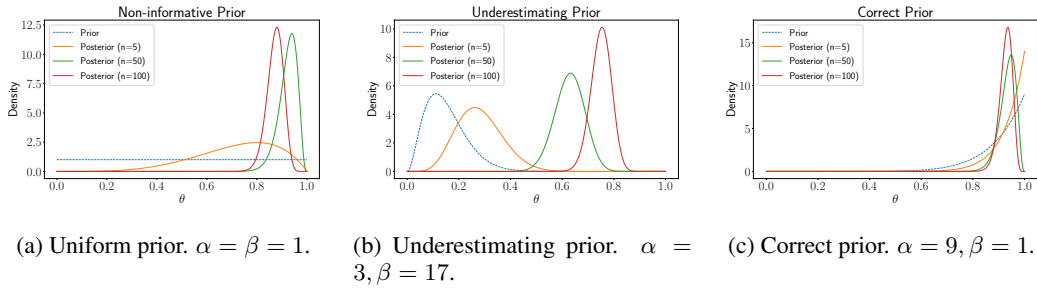


Figure 4: Different shapes of the posterior distributions.

M.2 PRIOR MISSPECIFICATION

In this section, we demonstrate, how the metrics of epistemic uncertainty behave, given different (possibly misspecified) priors. We present the results in Figure 5. We see, that as we discussed above, these metrics depend on the values of α and β . Therefore, the more these values are, the less is the estimate of epistemic uncertainty. Since uniform prior contains minimal evidence, it demonstrates maximal uncertainty, and therefore less vulnerable for prior misspecification. Note, that in our experiments on deep ensembles, we considered uniform prior over parameters, therefore the effect of prior misspecification should be negligible.

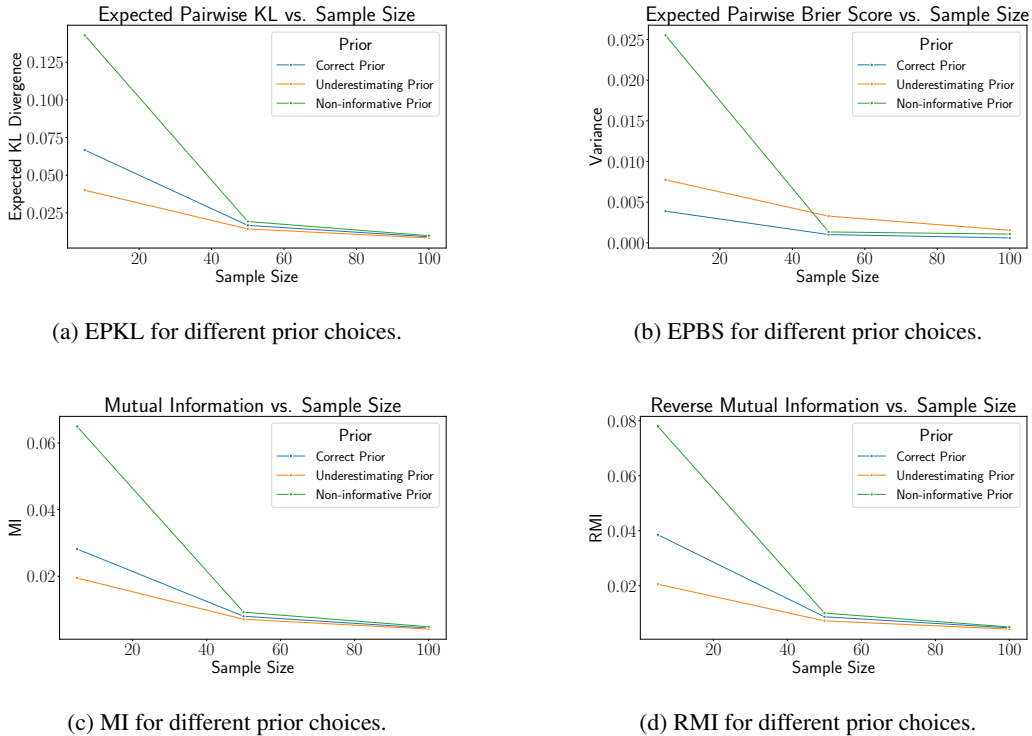


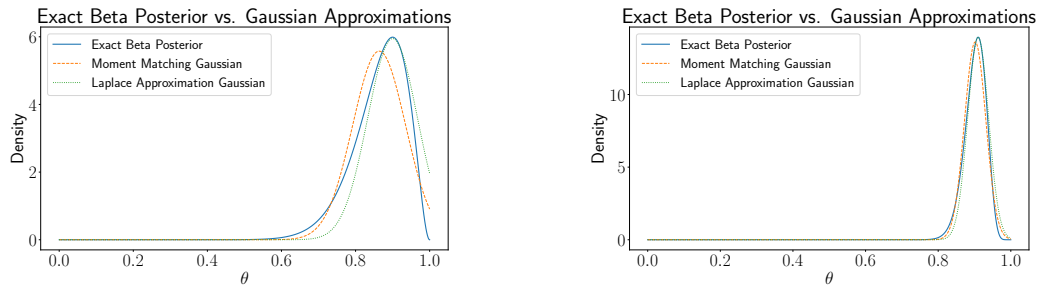
Figure 5: Epistemic uncertainty metrics, given prior misspecification and different samples sizes.

M.3 ERROR IN POSTERIOR APPROXIMATION

In this section, we consider the case of choosing wrong posterior distribution for inference. We know, that in our toy example, the correct family to consider for inference is Beta. However, we will misspecify the choice and consider Normal distribution instead. We use two approaches for

1944 inference. Namely, Laplace Approximation (approximates the posterior around the mode), and
1945 Moment Matching (matches the mean and variance of the Beta distribution with a Gaussian).
1946

1947 We present results in Figure 6. We considered uniform distribution as a prior, and we used training
1948 datasets of sizes 20 and 100. As expected, we see, that the given less data, errors in approximations
1949 are more severe. However, if a bigger dataset is provided, the approximation becomes more accurate.
1950



1951
1952
1953
1954
1955
1956
1957
1958
1959
1960
1961 (a) Approximations for $n=20$.

(b) Approximations for $n=100$.

1962
1963
1964
1965
1966
1967
1968
1969
1970
1971
1972
1973
1974
1975
1976
1977
1978
1979
1980
1981
1982
1983
1984
1985
1986
1987
1988
1989
1990
1991
1992
1993
1994
1995
1996
1997
Figure 6: Resulting approximations given different sizes of training datasets.